Investigation of Carboxylated Multi-Walled Carbon Nanotube Cytotoxicity In Vitro

A thesis presented in partial fulfilment of the requirements for the degree of

Masters of Science

In

Physiology

At Massey University, Palmerston North
New Zealand

Aaron David Gilmour

2010

Abstract

Carbon nanotubes have been idealised as carrier vehicles for cell targeted drug and gene delivery. The physiochemical properties of the carbon nanotube also promote its function as a 'thermal antennae' for non-invasive cancer destruction. Covalent modification of carbon nanotubes is a result of acidic purification resulting in carboxylated carbon nanotubes. Additionally this covalent modification allows for the attachment of biological moieties for cell targeting. Conversely, carboxylated carbon nanotubes are suggested to be cytotoxic to mammalian cells. The current study investigates the potential cytotoxicity of short, carboxylated, multi-walled carbon nanotubes in vitro, in a primary fibroblast cell culture model. Cytotoxicity is assessed with vital staining using propidium iodide, and secondly with a lactate dehydrogenase colorimetric assay. Results indicate that there is a dose dependent cytotoxic relationship between the carboxylated multi-walled carbon nanotubes tested and the fibroblast cell culture model.

Acknowledgements

First of all to my mum, thank you so much for supporting and encouraging me for all these years, and putting up with my endless supply of complaining, you're the best. Love you lots. And to my siblings, Laura, Shawn, Nigel and Sarah, you four are simply fantastic.

Second, I would like to thank my supervisors,

Christine Thomson, for your continued help, support, and wealth of knowledge.

Ashton Partridge, for the good laughs, and help with all things chemistry.

Craig Johnson, for your support and occasional good laughs

Again thanks, you are all awesome supervisors to have.

Third I would like to thank Sarah Taylor, for teaching me the basics of cell culture and showing me the joys of growing fibroblasts, and for being an awesome friend.

Krishanthi Jayasundera thanks so much for you help and guidance in the chemistry lab, and for all your helpful ideas and suggestions with those darn nanotubes.

Lastly to my many friends and flatmates, for putting up with my day to day grandpa-ness, my continual nerd talk, and listening to my endless supply of verbal rubbish. You guys are fricken awesome and super choice.

So thank you to all mentioned, you have all made this journey a possible, enjoyable and fascinating experience, I have learnt a lot.

Cheers

Aaron

Table of Contents

Abstract I
Acknowledgements II
Table of Contents III
List of Figures IV
List of Tables VI
Abbreviations VI
1. Introduction 1
1.1 Carbon Nanotubes 2
1.2 In Vitro Cell Culture Models 7
1.3 Nanotoxicology and In Vitro Cytotoxicity Assays 8
1.4 Aims and Objectives 10
2. Materials and Methods 14
2.1 Carbon Nanotubes 14
2.2 Cell Culture 17
2.3 Methods for Assessing ppMWCNT Cytotoxicity 21
3. Results 27
3.1 Carbon Nanotubes 27
3.2 Primary Cell Culture 30
3.3 Cytotoxicity Assays 31
4. Discussion 37
4.1 Effect of ppMWCNT on Cell Viability 37
4.2 Suspending Carboxylated Multiwalled Carbon Nanotubes 38
4.3 Fibroblast Cell Cultures 41
4.4 Cytotoxicity Assays 41
5. Conclusion 45
6. References 47
Appendix 1 52
1.1 Recipes for Cell Culture Media 52
1.2 Fixatives and Stains 53
1.3 Poly-L-Lysine (PLL) Coating of Coverslips 54

List of Figures

Figure 1.1 *Schematic diagrams of A) seamless cylinder model of CNT, B) graphene sheet with basic outline of CNT, C) cut multi-walled CNT showing concentric tubes, D) three orientations of carbon rings along the axial plain of the CNT.* 4

Figure 2.1 *24 well plate layout for LDH activity assay* 26

Figure 2.2 *96 well plate layout for LDH activity assay* 26

Figure 3.1 Representative images of COOH-CNT (A) and ppMWCNT (B). Suspensions for both NanoLab COOH-CNT and ppMWCNT were prepared at 1mg/ml; samples for TEM were taken from the upper 1/3 of the suspension to avoid any large aggregates. The images depict the difference in solubility between the two nanotube types as the density of CNT in the COOH-CNT is less than ppMWCNT. Secondly, ppMWCNT also have shorter lengths and less CCF (white arrows) present. The black arrow indicates artefacts on the TEM image and the circles indicate CRaP. 28

Figure 3.2 Panels A-D are representative images of 'as purchased' COOH-CNT suspensions as resulted initially from methods 1-4 respectively panels F-I are the same suspensions after 30 minutes. Panels E and J are the initial and 30 minute images of the ppMWCNT sample. All samples were suspended at 1mg/ml. Panels A and F are in 50% FBS, B and G are in 1M NaOH, C and B resuspended in 10% FBS in DMEM, and D and I were diluted to 50% with DMEM. 29

Figure 3.3 ppMWCNT suspension at 1mg/ml in FFM 10% three months after sonication. The suspension was relatively stable although a small amount of visible sediment accumulated on the bottom of the glass scintillation vial. 30

Figure 3.4 Primary culture of mouse skin fibroblast (A) at 2-3 days depicts outgrowth of cells from the skin explant (white arrow) and (B) the culture at 13-14 days depict the cells at approximately 75% confluence. 30

Figure 3.5 ppMWCNT forming a thin film over DAPI stained nuclei causing a dark shadow. Representative shadowed nuclei are indicated by the white arrows 31

Figure 3.6 The photomicrograph shows ppMWCNT have adsorbed and emit a red fluorescence (white arrows) characteristic of PI. The image also shows dead fibroblast nuclei (intensely stained red spheres. Inset is an enlargement of ppMWCNT fluorescing red from PI adsorbance. 32

Figure 3.7 Effect of ppMWCNT concentration on the viability of mouse skin fibroblasts. Bar graph with error bars show the overall effect of increasing ppMWCNT concentration with a trend towards a loss of cell viability (** indicates P=0.001 and * P=0.05 as compared with 0µg/ml). The individual lines represent the mean change in live/dead cell ratio for the three repeats of the experiment. The yellow line ends at 80µg/ml due to a processing error causing 100% cell death across all coverslips in that experimental trial. Values were corrected relative to 0µg/ml = 100% cell viability. 33

Figure 3.8 Effect of ppMWCNT concentration on the presence of LDH in FFM 10% (results of pilot study 2). The solid line represents FFM 10% + LDH + ppMWCNT (positive control), the dotted line FFM 10% + ppMWCNT (negative control), and the dashed line (difference of controls) is the product of subtracting the negative control from the positive control (all media was filtered before LDH assay was conducted except for the 0µg/ml sample. This graph indicates that ppMWCNT had no effect on LDH levels or the LDH assay. 34

Figure 3.9 Figure A) is representative of the colorimetric change across the 96 well plate, refer to figure2.2 for contents of each well. Figures B and C are images of the media with 200µg/ml ppMWCNT before (B) and after (C) filtering 35

Figure 3.10 Effect of increasing ppMWCNT on LDH levels in cell culture media (FFM 10%). Bars graph with error bars indicates the overall effect of increasing ppMWCNT concentration on the release of intracellular LDH into the cell culture media (* indicates P=0.05 and ** indicates P=0.001). The line graphs are data from individual experimental trials. Values are corrected relative to 0µg/ml=0% increase in LDH. 36

Figure 4.1 Schematic representation of CNT with proteins adsorbed to outer surface (A) and the wrapping of individual proteins around CNT (B). Figure 'A' is modified from Wallace, et al. (2010)[70] and Figure' B' is modified from Matsuura, et al. (2006)[43]. 39

Figure 4.2 Schematic of the reaction of COOH-CNT with NaOH. Dispersing COOH-CNT in a 1M NaOH solution changes the COOH terminal to COO^-Na^+ making the terminal non-polar and subsequently reducing the hydrophobic nature of the COOH-CNT 39

Figure 4.3 Schematic representation of a SWCNT surrounded by carboxylated carbonaceous fragments (CCF). Upon reflux with 1M NaOH, the OH terminal is changed to O^-Na^+ which solubilises the fragments in the NaOH solution. 40

Figure 4.4 Schematic of a benzene ring (A) and propidium iodide (B). The six membered carbon commonly referred to as a benzene ring is the necessary component making a compound aromatic i.e. contains at least one benzene ring structure. The schematic of propidium iodide indicates that it contains more than one benzene ring therefore making it an aromatic compound..... 43

List of Tables

Table 1.1 Summary of previous in vitro nanotoxicological research with carbon nanotubes 12

Table 3.1 Descriptive statistics for percentage viable cells as assessed by DAPI/PI staining..... 32

Table 3.2 Descriptive statistics for changes in cell viability as assessed by LDH assay 35

Abbreviations

CCF	Carboxylated Carbonaceous Fragment
CNT	Carbon Nanotube
Co	Cobalt
COOH-CNT	Carboxylated Carbon Nanotube
COOH-MWCNT	Carboxylated Multi-Walled Carbon Nanotube
CRaP	Carbonaceous Residues and Particles
Cu	Copper
CVD	Chemical Vapour Deposition
DAPI	4,6-Diamidino-2-phenylindole
ddH2O	Double Distilled Water
DMEM	Dulbecco's Modified Eagles Medium
ELISA	Enzyme Linked Immunosorbent Assay
FACS	Fluorescence Assisted Cell Sorting
FBS	Fetal Bovine Serum
Fe	Iron
FFM	Fibroblast Feeding Medium
H_2SO_4	Sulphuric Acid
HAEC	Human Aortic Endothelial Cells
HBSS	Hanks Balanced Salt Solution
HNO_3	Nitric Acid
LDH	Lactate Dehydrogenase
Mo	Molybdenum
MWCNT	Multi-Walled Carbon Nanotube
Ni	Nickel
PBS	Phosphate Buffered Saline
PI	Propidium Iodide
PLL	Poly-L-Lysine
ppMWCNT	Post-Processed Multi-Walled Carbon Nanotube
RCF	Relative Centrifugal Force
SWCNT	Single-Walled Carbon Nanotube
TEM	Transmission Electron Microscope

1. Introduction

The fields of nanoscience and nanotoxicology are two relatively young areas of research. The primary focus of nanoscience is the production, modification and study of nanoparticles. Nanoparticles are generally classified as any material with at least one dimension less than 100nm [34]. In contrast, the focus of nanotoxicology is to study the potential impacts of these unique nano-sized particles on animals and the environment. Of specific interest to the current study is the scientific discovery and characterisation of carbon nanotubes (CNTs) [30] in relation to their proposed use in biomedical applications [4, 36, 62].

Carbon nanotubes were first described in detail in 1991[30]; following from this, there has been an explosion of ideas regarding the use of CNTs. Adjacent to the explosion of ideas, has been a simultaneous explosion in the production of these materials [36, 45]. At a point in this short history CNTs were proposed as potential drug and gene carrier vehicles [27], and near infrared 'thermal antennae' for cancer destruction [21]. This introduction of CNTs into biomedical applications introduces the need to investigate possible interactions between CNTs and biological systems especially mammals. There are two principle reasons for studying the nanotoxicology of carbon nanotubes. First, is their potential use in biomedical applications, and second, are the industrial production and the potential effects for people handling these materials [25].

The specific form of carbon nanotube that is of interest in the current study are carboxylated, multi-walled CNTs (COOH-MWCNT). There are two reasons for choosing this specifically modified type of CNTs. The primary reason is that COOH (or carboxyl) group attached to the MWCNT can be used as a starting point for the covalent attachment of cell-specific targeting moieties, such as ligands, proteins, and hormones. The ability to modify MWCNT in such a way might allow for cell specific drug delivery [27]. The second reason, behind this choice, is the COOH group is a by-product of acidic purification of raw CNTs materials which, is one of the most commonly used procedures to remove metallic and carbonaceous impurities [34].

As with several other nanoparticles, there is concern about the materials' biocompatibility and the potential for COOH-MWCNT to have a cytotoxic fate in vivo and in vitro [38]. However, to assess the potential toxicity of CNTs there needs to be an

understanding of how their physiochemical properties make them an attractive target for biomedicine and a potential hazard to people and the environment [25].

1.1 Carbon Nanotubes

1.1.1 Structure of Carbon Nanotubes

The most basic model of a carbon nanotube can be visualised as a sheet of six-membered carbon rings rolled into a seamless cylinder [22], as shown in figure 1.1a. The single sheet of six-membered rings is commonly referred to as graphene (figure 1.1b) this is the singular sheet component of graphite [50]. This single layer is rolled into a tube of length '*OB*' with a circumference '*OA*' (notation refers to vector arrangements regarding CNTs orientation and parameters relating to the graphene sheet) (see figure 1.1b) [34]. The length and circumference of any CNT can vary depending on several parameters during growth [12]. There are two major types of CNTs. First, a single layer of graphene rolled into a tube resulting in a single-walled CNTs (SWCNT). Second, is a multi-walled CNTs (MWCNT) this is made up of two or more tubes wrapped around each other in a concentric manner (see figure 1.1c) [15].

Carbon nanotube properties vary significantly within the broad macrostructure of individual tubes. For example, the orientation of carbon rings with reference to the longitudinal tube axis (see figure 1.1d) can result in metallic or semiconducting SWCNT [42]. Metallic tubes are either arm-chair or zigzag by description, and semiconducting tubes are known as chiral, which includes all other orientations of the carbon rings (see figure 1.1d). This property can be overlooked in MWCNT as each individual concentric tube can have its own orientation, for example, the central tube might be zigzag, with the next tube being chiral and so on, in no particular order [54]. However, the diameter and length of SWCNT and MWCNT can have considerable effects on their electrical, mechanical, and bio-interactive properties [35, 60]. In addition to the macrostructure, the atomic structure of CNTs is unique and affects the overall CNT properties [15].

Carbon atoms can interact with each other in three ways depending on the morphology of the final structure. In brief, the quantum theory of the atom describes the relative positions of electrons relative to the nucleus of the atom, their energy level within an electron shell and their relative position to each other. The theory allows atoms to form

hybridized orbitals, where electrons from two different orbits combine forming a hybrid orbit. The relative position of electrons in their orbitals is annotated as follows: $1s^2$ $2s^2$ $2p^6$ $3s^2$ $3p^6$. Where the large number denotes the electron shell, the letter denotes the orbital (subshell) within the electron shell and the superscript number denotes the number of electrons present. Carbon has an electron structure in its ground (non-hybridised state) of $1s^2$ $2s^2$ $2p^2$. Hybridisation of the carbon atom occurs between the 2s and 2p orbital's (subshells) resulting in either sp^1, sp^2 or sp^3 bonding characteristics. sp^1 bonding occurs in acetylene (C_2H_2), where each carbon interacts with two other atoms. sp^2 bonding (planar) occurs when a carbon atom bonds to three other atoms as in graphene (see figure 1.1b). sp^3 (tetrahedral) bonding occurs in molecules such as methane (CH_4) and in the crystal structure of diamond, where each carbon bonds to four other atoms.

The hybrid bonding between carbon atoms in a CNT is significant in that it provides it with very unique properties. Normally 3D carbon structures like diamond are formed from tetrahedral (sp^3) bonding, however, CNTs are a 3D structure constructed of sp^2 bonds normally found in planar structures like graphene. There are a few simple principles that need to be noted in carbon-carbon bonding:

- When a bond is made, energy is released.
- The less potential energy remaining the greater the stability of the final structure
- Therefore, the more bonds that are made the more stable the final structure is, so the preferred bonding arrangement for carbon is sp3 (i.e. there is less potential energy remaining between atoms).
- Bonds are formed at the greatest possible distance from each other.

So CNTs are a 3D object created from a 2D (planar) bonding structure but have 1D characteristic's. The sp^2 bonding has higher potential energy between atoms compared to sp^3 bonds. For CNTs this results in a 1D structure with high potential energy with no free bonding points to allow release of this energy. This arrangement is responsible for the electrical conductivity of CNTs [54]. Additionally, the smaller the tube diameter the higher this potential energy is due to the strain placed on the bonds, which is generated by the reduced bond angles [50, 54]. The key aspects here are the 3D object constructed

from sp^2 bonding, the high potential energy between atoms, and the distorted bond angles, the relevance of which will be discussed in following paragraphs.

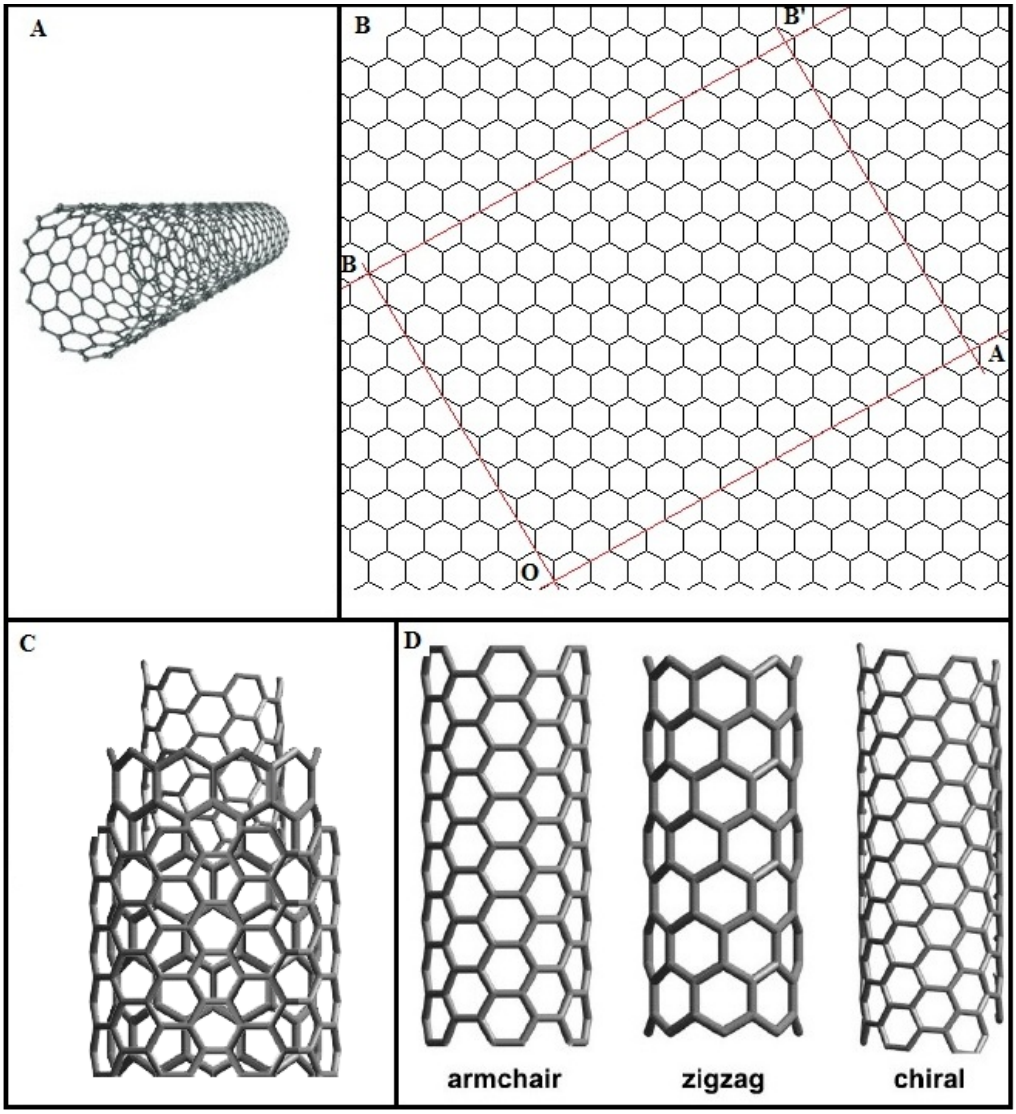

Figure 1.1 *Schematic diagrams of A) seamless cylinder model of CNT, B) graphene sheet with basic outline of CNT, C) cut multi-walled CNT showing concentric tubes, D) three orientations of carbon rings along the axial plain of the CNT.*

The high potential energy confined within the CNT structure causes pristine CNTs to be electrostatic. This electrostatic nature results in CNTs in the atmosphere being easily aerosolised [44], which with undefined toxicity is undesirable. Conversely, this same property significantly reduces the ability for CNTs to be homogenously dispersed in a surfactant free aqueous medium. The electrostatic charge results in the CNTs being hydrophobic therefore they have an innate tendency to aggregate within a liquid media [72]. This significant aggregation of CNTs within an aqueous media again is a highly undesirable property if they are to be used in biomedical applications, as large,

biopersistent aggregates of carbon causes inflammation and fibrosis as the immune system cannot remove the foreign material [47, 59].

It is commonly proposed that CNTs can act as 'thermal antennae' for non-invasive thermal destruction of cancer [65]. Carbon nanotubes can act as 'thermal antennae' because of the confined high potential energy between atoms [29, 55]. The application of near infrared light to carbon nanotubes causes excitation of the electrons resulting in the release of energy in the form of heat [55]. It has been shown that the specific heat of an excited CNT is sufficient to cause thermal destruction of adjacent mammalian cells [65]. In addition to thermal destruction of cells, open ends of CNTs are highly modifiable structures. Modification can be through covalent [16] or non-covalent [41] interactions. Furthermore, CNTs are able to have small molecules inserted into their inner cavity [26, 27]. Thus, CNTs appear to be highly attractive for biomedical applications. However, these same structural parameters lead to other properties that make CNTs undesirable for potential use in this area.

1.1.2 Purification and Functionalisation of Carbon Nanotubes

The purity, or the percentage, of the CNT that is carbon and is arranged in a uniform manner is thought to play a significant role in the potential reactivity of the CNT. In the first instance this is due to the presence of contaminating particles such as Fe, Co, Ni, Mo and Cu [51]. All these metals are catalyst particles used for CNT growth and production. They easily undergo oxidation and reduction reactions depending on their state, thereby providing a highly reactive surface of nanometer dimensions. Secondly, the potential reactivity is increased by the presence of carbonaceous residues and defects. These can be within, or attached to the hexagonal carbon lattice of the CNT wall [48]. Defects usually occur when there is a sp^1 or sp^3 bonded carbon atom within the wall resulting in bends and/or gaps [50]. These defects provide potential free electrons (dangling bonds). Dangling bonds are free chemical bonds associated with an atom in the surface of a solid, where the free electron extends to the exterior surface of the solid. Bonds of this form are susceptible to oxidation and provide free electrons that can interact with, or bind to, molecules carrying a charged portion [3], such as proteins. These defects result in the theoretically inert CNT surface being marginally, or highly reactive depending on the percent of defects present in a CNT sample [28].

Purification of CNTs aims to either reduce the number of defects and amorphous carbon and/or remove residual metal catalysts [18]. There are two methods commonly employed for purification of CNTs, first is thermal reduction, second is liquid phase acidic oxidation.

Thermal reduction involves heating CNT samples to temperatures of at least 400˚C under a pressurised vacuum. The pressurising gas is usually oxygen or hydrogen. The process causes annealing of CNT defects and amorphous carbon through thermal oxidation of weak carbon bonds. The process is reported to result in shorter, straighter, pristine CNTs as compared to the starting CNT sample. The most significant issue with this purification method is that it does not actively reduce metal catalysts [66].

In comparison, liquid phase acidic oxidation oxidises both CNTs at defect sites, and amorphous carbon. Additionally, the acid directly attacks, high oxidation potential metals causing rapid deterioration of residual catalyst metals. Two common acids, nitric acid (HNO_3) and sulphuric acid (H_2SO_4) are used either separately or in combination for this method. The acid oxidation treatment breaks CNTs at defect sites resulting in shorter, straighter CNTs with reduced metal catalyst contamination [39].

Acid oxidation results in ‘cleaner’ CNTs compared with thermal reduction due the reduction of catalysts metals. However, the oxidation process also introduces carboxyl groups (COOH) onto the outer-walls at defect sites and the tips of the CNTs [28]. When CNTs are acid oxidised, COOH groups also form on carbonaceous fragments and debris. These can be attached to the CNTs or free standing [58]. The presence of these carboxylated carbonaceous fragments (CCF) could interfere with the assessment of COOH-MWCNT cytotoxicity. In conjunction with this, CCF are thought to reduce the solubility of COOH-MWCNT in aqueous media [74]. Salzmann, et al. (2007)[56] indicates that washing COOH-MWCNT in a strong base solubilises the CCF, which can then be removed with filtration, leaving only larger particles, i.e. COOH-MWCNT [56].

The addition of carboxyl groups is a form of primary, covalent functionalization. Functionalization is the attachment of any molecule or compound to a CNT; this can be via covalent or non-covalent interactions. Covalently modified CNTs have irreversibly altered physiochemical properties, whereas non-covalently modified CNTs have their physiochemical properties masked [43, 70]. Non-covalent functionalization usually involves wrapping or coating the CNTs with a protein, synthetic molecule or surfactant.

Both forms of functionalization are indicated to increase the CNT solubility in non-polar aqueous media, for example cell culture media. The solubility of CNTs in cell culture media is directly relevant to the current study, as forming a stable, surfactant-free media will allow a direct dose-dependent study on the effects of adding COOH-MWCNT to cultured cells.

1.2 In Vitro Cell Culture Models

The toxicological assessment of novel nanoparticles is essential due to the increased production and potential applications in the area of biomedicine. Methodologies to investigate the relationship between nanomaterial and organisms can use either in vivo or in vitro models. Research to date using in vivo models indicates a strong relationship between CNTs and prolonged inflammation and fibrosis in tissues immediately in contact with the nanotubes [36, 47], such as, the lower respiratory tract. For this reason, a cell culture model for assessing the toxicity of low CCF COOH-CNTs is superior from an animal welfare perspective.

In vitro assessment of cytotoxicity can be achieved using a primary cell culture or a cell line. A primary cell culture is derived directly from live tissue dissected from an animal and can potentially have more than one cell type present, although, with successive subcultures a more uniform cell type can be achieved. In contrast, a cell line is loosely defined as an immortalized cell type which is generally well described. Cell lines are usually more robust with faster growth rates [20]. The use of cell lines allows for reproducibility of a toxicity model across laboratories. However, cell types present in most commercial cell lines whilst homogenous, are highly changed and no longer represent the parent tissue from which they were originally derived. Primary cells on the other hand are generally more sensitive to environmental change and are more closely representative of the parent cell type.

For the present study a primary, fibroblast cell culture model was chosen. Fibroblasts are representative of a non-tissue specific cell type that can be found widely distributed throughout the mammalian body. This cell type is generally more robust than tissue specific cell types, but as a primary culture, it is more sensitive to changes in its environment compared with a cell line [6].

1.3 Nanotoxicology and In Vitro Cytotoxicity Assays

Why is nanotoxicology of concern?

Nanotoxicology is an emerging field of research associated with the potential cytotoxic effects of particles which measure in the nanometer range. They include natural (e.g. mineral composites), incidental (e.g. diesel nanoparticles) and engineered (e.g. carbon nanotubes) materials. Nanotoxicity research to date gives strong evidence that these nano-sized materials have different toxicity profiles compared to macro-sized particles of the same composition. This difference is primarily due to the increased surface area, and their potential to access body cavities their larger counterparts cannot [49].

Potential Routes to Nanoparticle Induced Cell Death/Apoptosis

Biological and nano particles can interact with cells, in particular the cell membrane in three principle ways, surface interactions, endocytosis, or membrane penetration [49]. The type of interaction that might occur between the nanoparticle and the cell membrane is dictated by the parameters of particle size and shape (thus surface area) [23, 53, 57, 72], particle distribution state (dispersed or agglomerated) and their surface charge [10, 52]. The first two parameters function with regards to the potential number of reactive sites on the nanomaterial and the potential spaces they can occupy within a cell layer, tissue or organ. Surface charge of nanomaterials is implicated in how it might interact with the cell membrane. Primarily the phospholipid bilayer has net negative charge on the exterior of the cell. Therefore, nanoparticles with differing surface charges might have different effects at the cell membrane; in addition, the hydrophobic or hydrophilic nature of the material also has an effect here[40].

Interactions at the cell membrane can be by two mechanisms, first direct interactions with the membrane, this is most likely to occur with positively charged nanomaterials as indicated by Arvizo et al. (2010)[2] using gold nanoparticles (AuNP) with positive$^{(+)}$, negative$^{(-)}$, neutral or zwitterionic$^{(\pm)}$. Positively charged AuNP significantly altered the cell membrane potential altering intracellular Ca^{2+} levels. As suggested, positively charged nanoparticles (NPs) alter membrane characteristics [49] by affecting the nature of the lipid bilayer [2]. Second, NPs can interact with surface proteins with the potential to alter or block their function. These interactions could lead to altered cell function

resulting apoptosis or cell death, or allow entry of NP into the cell cytoplasm via mechanisms other than endocytosis.

Entry of NP into the cytoplasmic environment can occur via two mechanisms endocytosis or non-endocytic pathways [67]. Endocytosis can occur via pinocytosis in non-immune cells or phagocytosis in immune cells. Both mechanisms result in the foreign particle being engulfed by the cell membrane and moved into the cytoplasm within vacuoles. The fate of NP bound within vacuoles is unknown this includes the subsequent effects of these trapped NP. The resulting effect of NP within vacuoles is likely to be dependent on the purpose their inclusion into the cell. Macrophages phagocytise foreign bodies for breakdown and removal from the body, in the case of CNTs the stability of the atomic structure makes biological breakdown impossible therefore their subsequent removal unlikely. In vivo research with various CNT products suggests this is the case, the persistence of CNT within cytoplasmic vacuoles leads to an exacerbated immune response resulting in local inflammation and granuloma formation because of significant macrophage cell death [47, 59]. Interestingly in vitro research using A549 pneumocytes (non-immune cells) indicates inclusion of CNTs via pinocytic mechanisms, which generally function to include extracellular macromolecules required for cellular metabolism that cannot transverse the lipid bilayer by any other mechanism [60]. This indicates potential interactions with membrane proteins that regulate pinocytosis.

Further to surface and endocytic interactions of cells and NP, non-endocytic penetration of the cell membrane can occur. Arvizo et al. (2010)[2] found positively charged AuNP traversed the cell membrane of four cell types in vitro. Cell types include malignant ovarian cancer CP70 and A2780 cells, non-malignant, excitable human bronchial epithelial cells, and human airway smooth muscle cells. In addition, the positively charged AuNPs penetrated the cell membrane more easily compared to the other AuNPs. However, there is a small amount of evidence that suggests the size and needle shape of short (<500nm) CNTs enables them to easily penetrate the cell membrane, creating pores in the membrane resulting in cell death or apoptosis from the intracellular/extracellular ion balance being disrupted [67].

Methods for Assessing Nanotoxicology In Vitro

The emerging field of nanotoxicology is bringing with it a number of issues regarding the use of traditional and even modern cytotoxicity assays. For CNTs, the most significant issue is its apparent action as an organic adsorbent, interacting with molecules in solutions resulting in false positives and/or negatives depending on assay type. The most reported such interaction occurs between CNTs and the water insoluble MTT-formazan salt resulting in either over estimated readings [73] or false negatives [60]. Carbon nanotubes have also been noted to interfere with alamar blue [46] and Rhodamine B stains [1].

In light of these interactions, the current study employs two methods for the assessment of COOH-MWCNT toxicity; the first is a vital staining technique and second is a water-soluble, colorimetric assay.

Vital staining is the direct staining of living cultures to determine either the number of viable or non-viable cells present in a population. A counterstaining combination of propidium iodide (PI), which stains dead nuclei and DAPI, which stains all nuclei, was employed. This form of toxicity assessment looks at individual cells within a population to determine the ratio of live to dead cells

Conversely, a colorimetric assay determines the level of cell viability in an entire population of cells through measuring indicators of cell damage in the culture media. Lactate dehydrogenase (LDH) is a cytoplasmically located enzyme that is released into the media on disruption of the cell membrane. The LDH assay has previously been reported as not interacting with CNTs[73].

On an additional note, the use of surfactants for suspending CNTs of any type has been reported to alter their toxicity, most often reported to increase toxicity [14]. For this reason, surfactants have been avoided in the present study.

1.4 Aims and Objectives

There have been a number of studies conducted on the cytotoxicity of various derivatives of CNTs with the general conclusion that CNTs are cytotoxic. However, these studies have confounding factors, such as the presence of trace metals, variable size and agglomeration, carbonaceous defects and debris, and surfactants. To determine

the true toxicity of CNTs, we have undertaken a study using high purity, short, carboxylated carbon nanotubes with significantly reduced CCF. We have added these CNTs to cultured mammalian cells and assessed the subsequent cytotoxicity. Based on previous work in the area of CNT cytotoxicity it is hypothesised that short carboxylated CNT will have a dose dependent cytotoxicity (see table 1.1).

To achieve this goal, three specific sub-aims needed to be met. These aims were:

- To produce a stable, surfactant-free suspension of high purity, short, COOH-CNTs in cell culture media.
- To grow a durable, low maintenance, cell culture model of a widespread cell type.
- To validate two methods of assessing cellular viability/cytotoxicity for investigating COOH-CNTs cytotoxicity in vitro.

Table 1.1 Summary of previous in vitro nanotoxicological research with carbon nanotubes

Cell Type	CNT Type	Dimensions	Results	Method of Assessment	Ref.
Human osteoblastic line hFOB Human fibroblastic line HS-5	MWCNT	D = 10-15nm	Small decrease in cell viability of both cell lines (equivalent to polysulfone which is currently used in medicine) Additionally Collagen type-I secretion is enhanced by a polysulfone-MWCNT complex which is encouraging for tissue engineering	Collagen type-I secretion assay IL-6 Cell Titer 96 Proliferation Assay Free radical production	**Chlopek et al (2006)** [9]
Primary immune cells (mice lymphoid)	PEG fSWCNT (cycloaddition) PEG fSWCNT (oxidation/amidation)		No significant cell loss Both CNT types do not stimulate the proliferation of B-lymphocytes PEG fSWCNT (oxidation/amidation) stimulated macrophages to secrete TNFα and IL-6	Flow cytometry (annexin V and propidium iodide) DNA incorporated radioactivity assay TNFα and IL-6 ELISA	**Dumortier (2006)** [17]
HEK293 (human embryo kidney)	pSWCNT		Time and dose dependent decrease in cell viability	MTT assay	**Cui et al (2005)** [11]
T-lymphocytes (human) Jurkat T-leukemia (human)	Oxidised MWCNT	L = 1-5μm D = 20-40nm	Time and dose dependent decrease of cell viability of Jurkat cells	Trypan Blue exclusion Annexin V-FITC/Hoechst 33342 staining	**Bottini et al (2006)** [5]
THP-1 (human acute leukemia cell line) Wistar rats (6wks)	MWCNT	L = 220nm L = 825nm D = 20-40nm	In vitro both lengths produced dose dependent increase in TNF-α In vivo produced local inflammation in length dependent manner (825nm more toxic)	TNF-α Flexia assay In vivo inflammation assessment	**Sato et al (2005)** [57]
Human dermis fibroblasts (cell line)	SWCNT (purified)	L = 500nm D = 2nm	Dose and time dependent decrease in cell viability		**Tian et al (2006)** [64]
Human aortic endothelial cells (HAEC)	SWCNT MWCNT	SA = 641m^2/g SA = 56m^2/g	Dose dependent increase in cell death, as assessed by all assays.	WST-1 LDH cytotoxicity assay IL-8 detection assay	**Walker et al (2009)** [69]

			Marked disruption of actin and VE-cadherin cytoskeleton filaments after 24 hours	Actin and VE-cadherin visualisation	
A549 human pneumocytes	MWCNT	L = 0.1-12μm L = 0.1-3μm D=10-160nm	LDH and XTT indicated dose and time dependent increases in cell death MTT assay indicated cell death occurred at 1 hour post exposure to 7.5μg/ml TEM visualisation of cell sections after exposure indicated short MWCNT were internalized.	LDH cytotoxicity assay XTT MTT TEM – CNT localisation	**Simon-Deckers et al (2008)** [60]
MSTO-211H mesothelioma cell line	Raw CNT CNT agglomerates CNT bundles CNT pellets		All CNT types caused dose dependent decrease in cell viability (MTT) and cell proliferation (Hoechst 33258). Additionally agglomerated CNT were more cytotoxic than well suspended raw CNT	Hoechst 33258 MTT	**Wick et al (2007)** [72]
Chinese hamster lung fibroblast (V97) cells	SWCNT	D = 0.4-1.2nm	Trypan blue exclusion assay indicated time and dose dependent increases in cell death. COMET and micronucleus assays indicated a non-significant increase in DNA damage. The salmonella assay did not respond to the presence of SWCNT	Trypan blue assay COMET assay Micronucleus assay Ames Salmonella assay	**Kisin et al (2007)** [33]
Human epidermal keratinocytes (HEK)	MWCNT		MWCNT were visualised within cytoplasmic vacuoles. The neutral red assay indicated a slight dose dependent increase in cell death. Further IL-8 increased in a time dependent manner	TEM – CNT localisation Neutral red assay IL-8 detection assay	**Monteiro-Riviere et al (2005)** [46]
Splenic B-cell Bal17 (B-lymphoma cells)	Poly-L-lysine functionalised CNT		No decrease in viability for either cell type.	Flow cytometry (propidium iodide, annexin V-Cy5 and green fluorescent protein)	**Cai et al (2008)** [7]
A549 human pneumocytes	SWCNT with 10wt.% iron	D = 0.8-1.2nm	CB and Alamar Blue indicated dose dependant increases in cell death for SWCNT concentrations of 400-800μg/ml whereas MTT indicated significant toxicity at 3.12μg/ml	MTT Coomassie Brilliant Blue 250 (CB) Alamar Blue	**Davoren et al (2007)** [13]

Abbreviations: TEM – transmission electron microscopy, IL – interleukin, PEG – poly(ethylene glycol), LDH – lactate dehydrogenase, pSWCNT – pristine SWCNT, fSWCNT – functionalised SWCNT, L – length, D – diameter, SA – surface are

2. Materials and Methods

2.1 Carbon Nanotubes

Carboxylated multiwalled carbon nanotubes (COOH-CNTs) were obtained from NanoLab (Newton, Massachusetts) [PD15L1-5-COOH, Lot# 41709]. Carboxylated CNTs were specified by the manufacture as being 95% pure (as assessed by Thermogravimetric Analysis) and to range in length from 1μm to 5μm with an outer diameter of 15±5nm.

2.1.1 Suspending CNTs in Surfactant Free Media – Pilot Studies

Pilot trials were undertaken to assess if the COOH-CNT purchased from NanoLab could be suspended in a cell culture media (see Appendix 1.1) without the use of surfactants. Methods 1-4 outlined below looked at different media combinations and the effect of non-covalent modification of the COOH groups to improve COOH-CNT dispersion.

Note: All sonicating of CNTs suspensions was carried out at room temperature using a Sonorex 10P Ultrasound bath (Bandelin, Berlin, Germany) set at 100% power

Method 1

To assess if and at what concentration COOH-CNTs (NanoLab) could form a stable suspension in fibroblast feeding medium (see Appendix 1.1).

1. 0.5-1mg of COOH-CNTs (NanoLab) was added in 500μl of Dulbecco's Modified Eagles Medium (DMEM) (GIBCO, Invitrogen) with 2%, 10% or 50% fetal calf serum (FBS) (GIBCO, Invitrogen, NZ), or in 100% FBS.
2. Suspensions were sonicated in ultrasound bath for 20-30 minutes.

Method 2

To assess the effect of NaOH on forming a homogenous suspension of COOH-CNTs through the formation of Na salts with COOH groups on the CNTs.

1. 1-2mg of COOH-CNTs was added in 500μl of 10, 20, 30, 50 or 100% 1M sodium hydroxide (NaOH) (BDH Laboratory Supplies, London, England) in Milli-Q water.
2. Suspensions were sonicated in ultrasound bath for 20-30 minutes.

Method 3

To assess if the formation of Na salts on the COOH groups was stable and affected later solubility in fibroblast feeding media or fetal calf serum.

1. 1-2mg of COOH-CNTs was added in 500µl 1M NaOH
2. Suspension was sonicated in ultrasound bath for 20-30 minutes.
3. Suspension was centrifuged for 5 minutes in a micro centrifuge (Spectrafuge Mini C1301, Labnet International inc., Woodbridge, NJ, USA).
4. NaOH was decanted.
5. Remaining MWCNT were resuspended in 1ml of 10% FBS in DMEM or 100% FBS.

Method 4

To assess the stability of NaOH treated COOH-CNTs (method 2) suspension when diluted with DMEM (major component of cell culture media).

1 0.5-1mg of COOH-CNTs was added in 50, 100, 150, or 200µl 1M NaOH.

2 Suspension was sonicated in ultrasound bath for 20-30 minutes.

3 Suspensions were diluted with DMEM to make final volume 500µl.

4 Sonicate in ultrasound bath for 20-30 minutes.

2.1.2 Post Processing of CNTs

The ‘as purchased’ COOH-CNTs were modified using a chelating, cleaning and functionalisation protocol. Post processing aimed to increase COOH-CNT solubility in surfactant free media by reducing carboxylated carbonaceous fragments (CCF) and carbonaceous residues and particles (CRaP) (personal communication A. Partridge, 2009), and reducing COOH-CNT length. Post-processing was carried out in the Nanomaterials Research Centre laboratory (Massey University, New Zealand). The following method was modified from Salzmann et al. (2007) [56]

1. COOH-CNT were weighed and placed in 10M NaOH at a concentration of 10mg/ml.
2. COOH-CNT were sonicated for 20 minutes.

3. COOH-CNT suspension was refluxed for 48 hours at 100°C. Refluxing with NaOH was repeated until a clear supernatant was present before washing.

Note: Refluxing allows the addition of energy to a reaction in the form of heat for an extended period without the loss of reactants through evaporation.

4. Refluxed COOH-CNTs were centrifuged [RCF = 650g] using a MLW T52.1 bench-top centrifuge (Clandon Scientific, Farnborough, UK), and supernatant was removed, an equivalent volume of Milli-Q water was added to wash the CNTs; this was repeated 4x.

5. The CNT product was vacuum filtered with excess Milli-Q water using 0.45μm pore filter paper (Millipore, Billerica, MA, USA) until filtrate pH≈7.0±1.5.

6. The remaining CNT product was then dried at 60°C in a Contherm oven series 5 (Contherm, Wellington, NZ).

7. The dried CNT product was weighed and transferred to a clean reflux bulb with 69% nitric acid (HNO_3) at concentration of 5mg/ml.

8. CNT suspension was sonicated for 20 minutes.

9. Suspension was refluxed at 100°C for 24 hours.

10. Steps 4 and 5 were repeated

11. The remaining CNT sample was dried then weighed. The CNTs collected contained COOH groups, as did the starting CNT sample therefore these CNTs will be referred to as post-processed CNTs (ppMWCNT).

ppMWCNT Disinfection and Suspension in FFM 10%

1. 10 μg of ppMWCNT were placed in a 30ml glass scintillation vial and lightly wetted with a spray 70% ethanol/H_2O

2. Wetted ppMWCNT were left to dry uncovered in a PC2 biological cabinet for 14 hours under UV light.

3. The ppMWCNT were then suspended at 1mg/ml in fibroblast feeding media (FFM 10%) see appendix 1.1.

Transmission Electron Microscopy (TEM)

Transmission electron microscopy (TEM) was carried out to assess CNT length, dispersion and morphology.

1. CNT samples were suspended in 10% fetal calf serum (GIBCO, Invitrogen, NZ) in Milli-Q water at 0.25-1mg/ml.
2. Samples were sonicated in an ultrasound bath for 20-40 minutes.
3. A drop of CNT suspension was placed on parafilm "M" and a copper formvar grid was inverted and placed on top of the suspension and left for 5 minutes.
4. The grids were removed and touched to the edge of filter paper to remove excess fluid and allowed to air dry.
5. The grids were then viewed under a Philips CM10 TEM (Eindhoven, Netherlands). Images of CNTs were captured with Morada 11 mega-pixel digital camera (Olympus, Munster, Germany) using SIS iTEM software (Olympus, soft imaging systems, Munster, Germany).
6. CNT lengths were manually measured in Adobe Photoshop CS4 (Adobe Systems Incorporated).

2.2 Cell Culture

Animal Ethics

Mice were bred and euthanized in accordance with Massey University Animal Ethics Committee (MUAEC) guidelines.

2.2.1 Primary Fibroblast Cell Culture

Mouse fibroblasts were cultured as a model of a ubiquitous cell type suitable for assessing the potential toxicity of COOH-CNTs in vitro.

Mouse Skin Fibroblasts

1. Neonatal (<24 hour old) male Swiss mice (Plant and Food Research, Palmerston North, NZ) were euthanized by decapitation.
2. The body of the mouse was wetted with 70% ethanol/H_2O and gently blotted on tissue paper.

3. Sections of skin approximately 1cm^2 were dissected from the ventrolateral aspect of the abdomen under a Leica EZ4 Stereomicroscope (Leica, Germany). Care was taken to remove sub-dermal tissue to minimize culturing contaminating cell types.

4. The dissected sections of skin were placed into ice-cold DMEM 4500mg/ml glucose (GIBCO, Invitrogen).

5. Skin sections were transferred to sterile laminar flow hood (Biological safety cabinet class II, Email Westinghouse Pty Ltd, NSW, Australia) and using a surgical scalpel blade (Swann Morton, Sheffield, England) skin sections were cut into 1-2mm^2 squares.

6. The base of 35mm sterile tissue culture plastic Petri dishes (NUNC, Thermo Fisher Scientific, Denmark), were pre-wetted by flooding with DMEM and then removing most of the media.

7. The 1-2mm^2 squares of tissue were transferred into the Petri dishes prewetted with FFM 10%.

8. Approximately 5-6 sections were distributed over each Petri dish.

9. 100µl of Fibroblast Feeding Media 10% (FFM 10%) was added carefully to each Petri dish.

10. Petri dishes were placed in an incubator (Heracell 240, Thermo Scientific, MA, USA) for 30 minutes in a humidified atmosphere at 37°C with 5% CO_2.

11. At 30 minutes, a further 200µl of FFM 10% was added to each Petri dish, and then returned to incubator.

12. At 60 minutes, 200µl FFM 10% was slowly added to each Petri dish to make total volume 500µl per dish, and returned the incubator.

13. At 120 minutes, 200µl FFM 10% was slowly added to each Petri dish to make total volume 700µl per dish, and returned the incubator.

14. At 150 minutes, 300µl FFM 10% was slowly added to each Petri dish to make total final volume 1ml per dish, and returned the incubator.

Explant cultures were fed on a maintenance regime until a confluent monolayer was present in the 35mm petri dish, at which point the cells were passaged (see section 2.2.2 below) and transferred to two T25 tissue culture flasks (Cellstar, Greiner Bio-One, Germany).

2.2.2 Maintenance of Cell Cultures

All media and Trypsin added to cell cultures was pre-warmed to 37˚C in a waterbath (NÜVE NB20, Turkey). Cell cultures were kept in a Heracell 240 incubator (Thermo Scientific, MA, USA) with humidified atmosphere at 37°C with 5% CO_2.

Feeding Cell Cultures

During maintenance, cultures were fed three times per week by replacing 90% of FFM 10% in the petri dishes/cell culture flasks. Cells that had just been revived from -80°C were fed FFM 40% daily for the first 2 days. After the initial period the media was changed to FFM 10% and maintenance feeding regime was followed.

Passaging Cell Cultures

Cell cultures were passaged when cell confluence reached ≈ 80%; this was generally once a week.

1. All media was removed from the petri dish or culture flask and discarded.
2. 2ml (T25 flask = 25cm^2 growth surface) or 4ml (T75 flask = 75cm^2 growth surface) 0.5% Trypsin with EDTA (ethylenediaminetetraacetic acid) liquid (GIBCO, Invitrogen) was added to each culture dish.
3. Cultures were incubated for 5 minutes or until cells detached.
4. An equivalent volume of FFM 10% was added to inactivate trypsin.
5. The cell suspension was removed from the flask and placed into a centrifuge tube.
6. Cell suspensions were centrifuged (Functionline Heraeus Labofuge 400, Thermo Electron Corp. MA, USA) at RCF = 1700g for 5 minutes.
7. The supernatant was removed with 3ml sterile, plastic, transfer pipette.
8. The cell pellet was resuspended in FFM 10% to required cell concentration.

9. Resuspended cells were transferred to a new growth surface either tissue culture flask (NUNC) 1ml cell suspension: 9ml fresh FFM 10% [T75=65,000-70,000cells/ml] or 100µl cell suspension onto glass coverslips [30,000 cells/ml] (VWR international, Leicestershire, England).

10. These cultures were subsequently feed at 24 hours, after which the standard maintenance feeding regime was followed.

Cryo Freezing Cell Cultures

1. All media was removed from a 75mm^2 culture flask and discarded.

2. 4ml 0.5% Trypsin with EDTA (ethylenediaminetetraacetic acid) liquid (GIBCO, Invitrogen) was added to each culture.

3. Cultures were incubated for 5 minutes or until cells became detached.

4. An equivalent volume of FFM 10% was added to inactivate trypsin.

5. The cell suspension was removed from the flask and placed into a centrifuge tube.

6. Cell suspensions were centrifuged at RCF = 1700g for 5 minutes.

7. Supernatant was removed with 3ml sterile, plastic, transfer pipette.

8. The cell pellet was resuspended in 10ml of cell freezing media (see appendix 1.1) by gentle aspiration with a pipette.

9. 1ml of cell suspension was transferred to each cryotube (NUNC) and placed in Mr Frosty (Nalgene, Thermo Fisher Scientific, Denmark) in -80˚C freezer.

10. Cryotubes were left in the -80˚C freezer for at least 2.5 hours, and then moved to liquid nitrogen Dewar for storage.

Reviving Cryo Stored Cell Cultures

1. 4ml FFM 40% was placed in a T25 cell culture flask (see Appendix 1.1)

2. Cryotubes were removed from liquid nitrogen Dewar and placed in water bath at 37˚C

3. Immediately after thawing the cell suspension was transferred into a T25 flask

4. The reviving cells were placed in an incubator at 37˚C and 5% CO_2

2.3 Methods for Assessing ppMWCNT Cytotoxicity

2.3.1 Live/Dead Cell Staining

ppMWCNT Exposure and Cell Staining

1. Fibroblast cells were seeded onto poly-L-Lysine (PLL) (Sigma Aldrich) coated, sterile, 13mm round glass coverslips (VWR international, Leicestershire, England) (refer appendix 1.3 for PLL coating procedure) in a 24 well plate (Jet Bio-Chemicals INT'L., INC, Canada) at 30,000 cells/ml [total volume 600µl/well], and cultured overnight in incubator at 37°C, 5% CO_2.
2. The next day FFM 10% was discarded and was replaced with FFM 10% containing ppMWCNT at different concentrations, in triplicate.
3. COOH-CNT treated fibroblast cultures were incubated for 6 hours at 37°C, 5% CO_2.

The following COOH-CNT concentrations were used

1. 0µg/ml
2. 5µg/ml
3. 20µg/ml
4. 40µg/ml
5. 80µg/ml
6. 200µg/ml
7. 500µg/ml

4. Following the 6 hour incubation the ppMWCNT in FFM 10% was discarded and living cultures were rinsed briefly with pre-warmed Hanks Balanced Salt Solution (HBSS) with cations (Invitrogen).
5. Excess HBSS was discarded and cover slips were removed from wells and placed on small pedestals and 50-100µl of HBSS was applied.
6. The HBSS was removed and 50-100µl PI working solution (see Appendix 1.2) was applied, samples were incubated for 10 minutes at room temperature.
7. Excess PI solution was removed and samples rinsed 2x with HBSS for 2-5 minutes.
8. Samples were fixed using 4% paraformaldehyde (BDH Laboratory Supplies, London, England) in PBS for 10 - 15 minutes at room temperature.
9. Samples were rinsed 3x with PBS for 2 minutes.

10. Following fixation, 50-100µl of DAPI working solution (see Appendix 1.2) was applied to each sample and incubated for 10 minutes at room temperature.

11. Excess DAPI solution was removed and samples rinsed 2x with PBS for 2-5 minutes.

12. The coverslips were briefly rinsed in ddH_2O and mounted cell side down on microscope slides using Citifluor AF1 (Citifluor Limited, London, UK) anti-fade mountant and the cover slip edges were sealed with clear nail varnish.

Data Acquisition and Image Analysis

Using an Olympus BX51 fluorescence microscope (Olympus Corporation, Tokyo, Japan) 10 consecutive, non-overlapping frames were captured at 20x objective from each sample for both DAPI and PI channels resulting in 20 images per coverslip. Photomicrographs were obtained with MagnaFire S99802 (Optronics, USA) digital camera using MagnaFire 2.0 software (Optronics, USA) in an 8bit grey scale Tiff file format.

Cell nuclei in each image were manually counted with assistance of the multi point selection tool and measure function in Image J (Version 1.42q, NIH, USA) software. Cell counts for each frame were entered into a Microsoft Excel 2007 spread sheet (Microsoft, USA) and the percentage live and dead cells per frame was calculated.

2.3.2 Lactate Dehydrogenase Activity Assay

Pilot Study 1

Pilot study 1 was undertaken to assess the effect of different concentrations of ppMWCNT in cell culture media on the absorbance values obtained from ELISA plate reader (PowerWave 340, BioTek Instruments Inc., Vermont, USA)

1. A 1mg/ml stock solution of ppMWCNT was freshly prepared in FFM 10% (see appendix 1.1).

2. In a 96 well plate the 1mg/ml stock solution was diluted to achieve triplicate samples with final concentrations of 200, 80, 40 and 5µg/ml in FFM 10%.

3. The absorbance of the plate was read at 50nm intervals over a wavelength range of 400-600nm in an ELISA plate reader.

Pilot Study 2

Results of pilot study 1 indicated the need to remove ppMWCNT from the cell culture media before the LDH assay could be used. Pilot study 2, addressed the potential effects of filtering the media on LDH in media, and the potential for ppMWCNT to interact with LDH and/or the reagents of Roche Cytotoxicity Detection Kit ^{plus} [LDH].

1. Fibroblast cells were seeded into 14 wells of a 24 well plate [tissue culture treated] (Jet Bio-Chemicals INT'L., INC, Canada) at 30,000 cells/ml in 600µl FFM 10% and incubated overnight at 37°C, 5% CO_2.

2. 15µl of lysis solution was added (Roche Cytotoxicity Detection Kit ^{plus} [LDH], Roche Diagnostics, Mannheim, Germany) to each well and the plate returned to incubator for 15-20 minutes.

3. All media was transferred to an appropriate sized sterile tube. This media was high in LDH due to induced cell lysis.

4. High LDH media was aliquoted into 5x300µl lots.

5. ppMWCNT suspended in FFM 10% was combined with high LDH media (from step 3) to a final volume of 600µl with ppMWCNT concentration

1.	Blank media (no lysis solution)*	6.	200µg/ml
2.	0µg/ml unfiltered **	7.	5µg/ml no LDH
3.	0µg/ml ***	8.	40µg/ml no LDH
4.	5µg/ml	9.	200µg/ml no LDH
5.	40µg/ml		

* Assess basal level of LDH present in FFM 10%
** Assess basal level of LDH in unfiltered media (with LDH added)
*** Assess basal level of LDH in filtered media (with LDH added)

The added LDH was collected from cultures where cell lysis had been induced using the lysis solution provided in the Roche Cytotoxicity Detection Kit ^{plus} [LDH]

6. All media was incubated at 37˚C in a waterbath for 2-3 hours

7. ppMWCNT were removed from the media by passing each sample through a separate, clean, 0.45µm syringe filter (Sartorius Stedim Biotech, Aubagne, France) into a clean 2ml eppendorf

8. The filtrate was aliquoted in 100µl lots in triplicate into a 96 well plate

9. 100µl of reaction mixture (Roche Cytotoxicity Detection Kit ^{plus} [LDH]) was added to each well

10. The plate was incubated at room temperature for 5-10 minutes

11. 50µl of Stop Solution was added to each well and absorbance measured at 492nm in an ELISA plate reader

Lactate Dehydrogenase Activity Assay

1. Fibroblast cells were seeded into 14 wells of a 24 well plate [tissue culture treated] (Jet Bio-Chemicals INT'L., INC, Canada) at 40,000 cells/ml in 600µl FFM 10% and incubated overnight at 37°C, 5% CO_2. (See Figure 2.1 for plate layout).

2. ppMWCNT in FFM 10% was diluted to the following concentrations

    1. 0µg/ml
    2. 5µg/ml
    3. 20µg/ml
    4. 40µg/ml
    5. 80µg/ml
    6. 200µg/ml
    7. 500µg/ml

3. Cell culture media was removed and replaced with 600µl of ppMWCNT in FFM 10% per well and incubated for 6 hours at 37˚C + 5% CO_2.

4. 600µl of FFM 10% containing the various concentrations of ppMWCNT was added to wells containing no cells (see figure 2.1). This media acted as the negative control.

5. 20µl of lysis solution from Roche Cytotoxicity Detection Kit ^{plus} [LDH] (Roche Diagnostics, Mannheim, Germany) was added to all wells in columns 2 and 5 of the 24 well plate and incubated for further 15-20 minutes at 37°C + 5% CO_2. (This was to induce maximum cell damage to produce positive controls)

6. Culture media containing ppMWCNT was removed from each well and placed in appropriate sized tube.

7. Recovered culture media was passed through separate 0.45µm pore sterile syringe filters (Sartorius Stedim Biotech, Aubagne, France) into clean 2ml eppendorfs, to remove excess CNT in the samples.

8. The filtrate from each sample was aliquoted in 100µl volumes, in quadruplet, into a 96 well plate (see Figure 2.2 for layout).

9. Using Roche Cytotoxicity Detection Kit ^{plus} [LDH], 100µl of reaction mixture was added to each well and the plate was incubated for 5-10 minutes in the dark.

10. 50µl of Stop Solution was added to each well.

11. The absorbance was measured at 492nm in ELISA plate reader (PowerWave 340, BioTek Instruments Inc., Vermont, USA) and output was recorded by Gen5 Microplate Data Collection & Analysis software (BioTek Instruments Inc., Vermont, USA).

12. Data was exported to a Microsoft Excel 2007 spreadsheet (Microsoft, USA).

Data Analysis

All data was transferred to SPSS 16 for Windows (SPSS inc. Chicago, Illinois, USA) data sheets. Data was converted to relative percentages of live/dead values for statistical analysis. Univariate analysis of variance and between samples t-tests were used to analyse the data.

	1	2	3	4	5	6
A	Cells 0µg/ml	Cells 0µg/ml	No Cells 0µg/ml	Cells 80µg/ml	Cells 80µg/ml	No Cells 80µg/ml
B	Cells 5µg/ml	Cells 5µg/ml	No Cells 5µg/ml	Cells 200µg/ml	Cells 200µg/ml	No Cells 200µg/ml
C	Cells 20µg/ml	Cells 20µg/ml	No Cells 20µg/ml	Cells 500µg/ml	Cells 500µg/ml	No Cells 500µg/ml
D	Cells 40µg/ml	Cells 40µg/ml	No Cells 40µg/ml			

Figure 2.1 *24 well plate layout for LDH activity assay*

	Experimental Cells + ppMWCNT				**Positive controls Cells + Lysis sol[n] + ppMWCNT**				**Media (negative) controls ppMWCNT**			
	1	**2**	**3**	**4**	**5**	**6**	**7**	**8**	**9**	**10**	**11**	**12**
A	0µg/ml	0µg/ml	0µg/ml	0µg/ml	0µg/ml	0µg/ml	0µg/ml	0µg/ml	0µg/ml	0µg/ml	0µg/ml	0µg/ml
B	5µg/ml	5µg/ml	5µg/ml	5µg/ml	5µg/ml	5µg/ml	5µg/ml	5µg/ml	5µg/ml	5µg/ml	5µg/ml	5µg/ml
C	20µg/ml	20µg/ml	20µg/ml	20µg/ml	20µg/ml	20µg/ml	20µg/ml	20µg/ml	20µg/ml	20µg/ml	20µg/ml	20µg/ml
D	40µg/ml	40µg/ml	40µg/ml	40µg/ml	40µg/ml	40µg/ml	40µg/ml	40µg/ml	40µg/ml	40µg/ml	40µg/ml	40µg/ml
E	80µg/ml	80µg/ml	80µg/ml	80µg/ml	80µg/ml	80µg/ml	80µg/ml	80µg/ml	80µg/ml	80µg/ml	80µg/ml	80µg/ml
F	200µg/ml	200µg/ml	200µg/ml	200µg/ml	200µg/ml	200µg/ml	200µg/ml	200µg/ml	200µg/ml	200µg/ml	200µg/ml	200µg/ml
G	500µg/ml	500µg/ml	500µg/ml	500µg/ml	500µg/ml	500µg/ml	500µg/ml	500µg/ml	500µg/ml	500µg/ml	500µg/ml	500µg/ml
H												

Figure 2.2 *96 well plate layout for LDH activity assay*

3. Results

3.1 Carbon Nanotubes

3.1.1 NanoLab COOH-CNT Characterisation

Carboxylated multi-walled carbon nanotubes (COOH-CNTs) obtained from NanoLab (Newton, Massachusetts) were specified as measuring 1-5μm in length with an average outer diameter of 15±5nm. The presence of elemental carbon was measured to be >95% as assessed by thermogravimetric analysis (TGA) [data obtained from manufacturer website www.nano-lab.com/cooh-functionalized-nanotubes.html].

The COOH-CNTs obtained from NanoLab when viewed under TEM in the present study had a large variability in length ranging from <1μm up to 7-8μm as can be seen in figure 3.1a. The general structural morphology of the COOH-CNTs was largely bamboo-like in appearance with at least one end capped. Additionally these COOH-CNT samples contained significant amounts of free and nanotube-bound carbonaceous residues and particles (CRaP).

3.1.2 COOH-CNT Suspension in Surfactant Free Media

Method 1 – Suspending COOH-CNT in different FBS concentration

After 30 minutes in the ultrasound bath COOH-CNT formed suspensions at all concentrations of FBS, but also contained variably sized agglomerates of COOH-CNT material in the bottom of the eppendorf. On visual inspection, COOH-CNT suspension appeared to be dependent on FBS concentration. The amount of COOH-CNT aggregates in the bottom of the eppendorf decreased with increasing FBS concentrations (see figure 3.2A).

Observations at 30 minutes post-ultrasound bath treatment indicated that COOH-CNT formed agglomerates and settled out of suspension at all FBS concentrations (see figure 3.2F).

Method 2 – Suspending COOH-CNT in NaOH

Immediately after 30 minutes sonication COOH-CNTs formed gel like suspensions in 50% and 100% 1M NaOH with no obvious agglomerates remaining in the bottom of the eppendorf. These suspensions appeared stable at 30 minutes post sonication (see figure

3.2B and G). COOH-CNTs in 10%, 20%, and 30% NaOH also formed well dispersed suspensions. However, at these NaOH concentrations, the COOH-CNTs agglomerated and settled out of suspension within 5 minutes post sonication.

Method 3 – Re-suspending NaOH treated COOH-CNT in FFM 10%

Within 1-5 minutes after sonication, NaOH treated COOH-CNTs quickly settled out of suspension at all FFM concentrations. However, the COOH-CNTs were not tightly agglomerated and were easy to re-disperse. This was an improvement over the previous method (see figure 3.2C and H).

Method 4 – Diluting NaOH treated COOH-CNT with DMEM

As previously indicated, COOH-CNTs sonicated for 30 minutes in 1M NaOH resulted in an even gel like suspension. On dilution with DMEM all suspensions were initially well dispersed, however, within 30 minutes post sonication the COOH-CNTs formed agglomerates and settled out of suspension (see figure 3.2D and I).

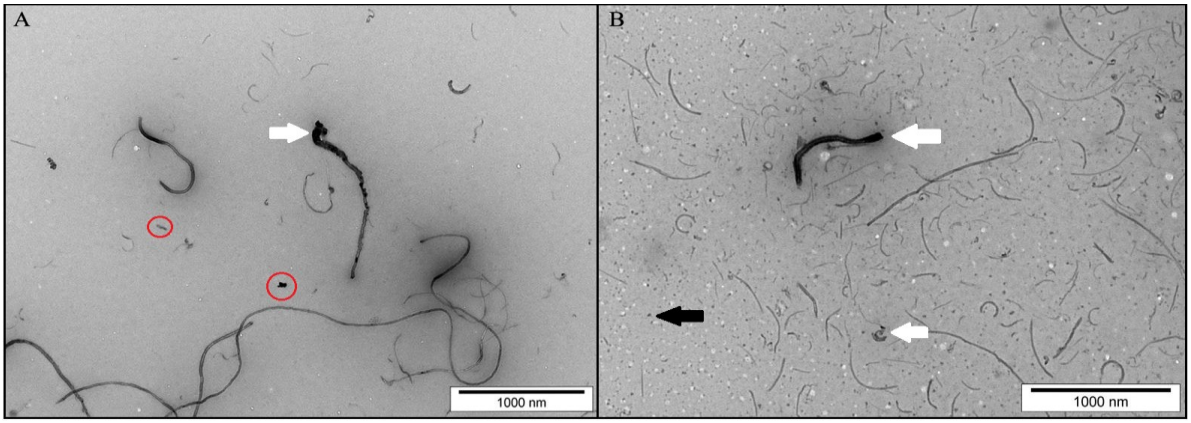

Figure 3.1 *Representative images of COOH-CNT (A) and ppMWCNT (B). Suspensions for both NanoLab COOH-CNT and ppMWCNT were prepared at 1mg/ml; samples for TEM were taken from the upper 1/3 of the suspension to avoid any large aggregates. The images depict the difference in solubility between the two nanotube types as the density of CNT in the COOH-CNT is less than ppMWCNT. Secondly, ppMWCNT also have shorter lengths and less CCF (white arrows) present. The black arrow indicates artefacts on the TEM image and the circles indicate CRaP.*

3.1.3 Post-Processed CNT (ppMWCNT) Characterisation

As a result of post processing with NaOH and HNO_3, the final length of ppMWCNT ranged from 150-1000nm with an average length of 502±251nm (n=180). Visually, there was a reduction in carbonaceous fragments. In addition, a reduction in the relative amount and size of CRaP in ppMWCNT TEM images was noted (see figure 3.1a and b).

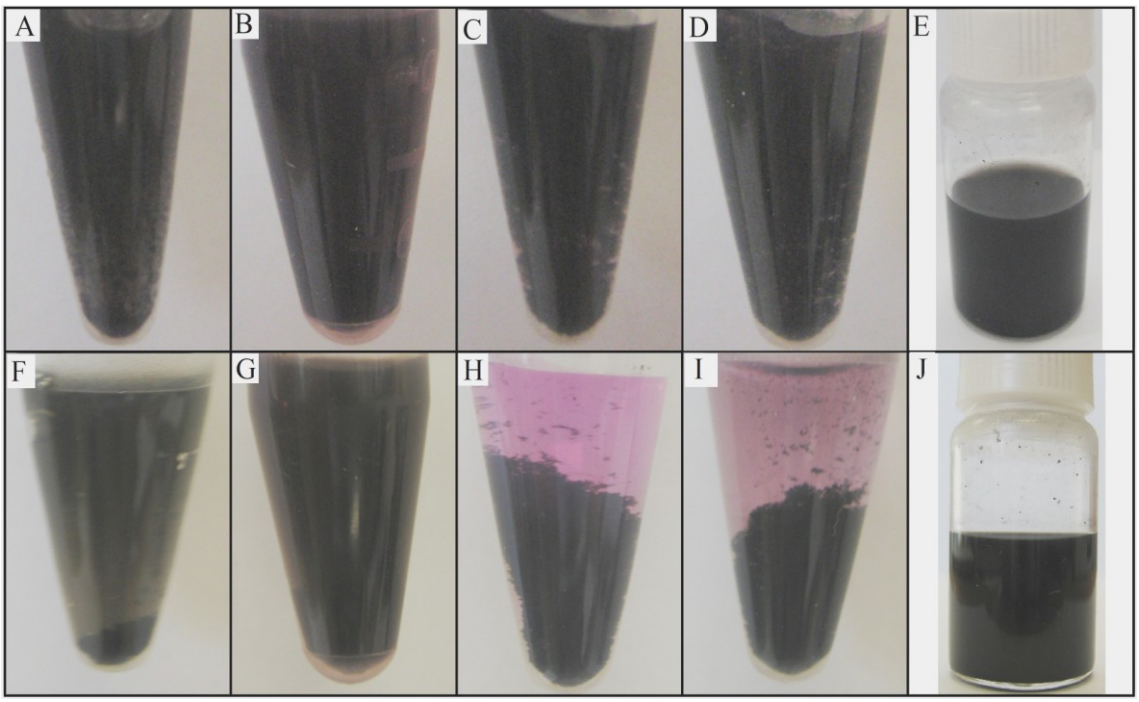

Figure 3.2 *Panels A-D are representative images of 'as purchased' COOH-CNT suspensions as resulted initially from methods 1-4 respectively panels F-I are the same suspensions after 30 minutes. Panels E and J are the initial and 30 minute images of the ppMWCNT sample. All samples were suspended at 1mg/ml. Panels A and F are in 50% FBS, B and G are in 1M NaOH, C and B resuspended in 10% FBS in DMEM, and D and I were diluted to 50% with DMEM.*

3.1.4 ppMWCNT Suspension in Surfactant Free Media

Following the post processing treatment of COOH-CNT with NaOH and HNO_3 (refluxing), ppMWCNT were suspended in FFM 10% at a concentration of 1mg/ml. Immediately after 30 minutes sonication in a glass scintillation vial a well dispersed suspension of ppMWCNT was observed with no obvious ppMWCNT sedimentation or agglomerates. At 30 minutes post sonication there were no observable changes in the ppMWCNT suspension (see figure 3.2E and J). An additional sample of CNTs that had undergone the NaOH washing but not HNO_3 was also suspended for TEM observation; this was initially well dispersed but formed large agglomerates after 12 hours in suspension.

The ppMWCNT suspension in FFM 10% was stored at 2-4˚C for 3 months. Visual inspection of ppMWCNT suspensions at three months indicated that the ppMWCNT were still well dispersed See figure 3.3), but there was a small amount of sedimentation. However, the sediment was easily re-suspended following 10 minutes sonication and remained in suspension for at least 12 hours.

In addition, after several months' storage in cell growth media (FFM 10%) there is no sign of contamination, this indicates the disinfection used was sufficient to eliminate possible sources of contamination.

Figure 3.3 *ppMWCNT suspension at 1mg/ml in FFM 10% three months after sonication. The suspension was relatively stable although a small amount of visible sediment accumulated on the bottom of the glass scintillation vial.*

3.2 Primary Cell Culture

The primary cell culture method used for this study was effective in producing durable and prolific mouse skin fibroblast cultures. Initial cell outgrowth from mouse skin explants was visible after 24 hours. The rate of fibroblast cell outgrowth after 24 hours was approximately 2-4mm per day (measurement refers to the limit of radial outgrowth from an individual skin explant), resulting in a 35mm Petri dish having a confluent monolayer of fibroblast cells in 14-17 days. Images in figure 3.4 are representative of fibroblast outgrowth at different stages of culture.

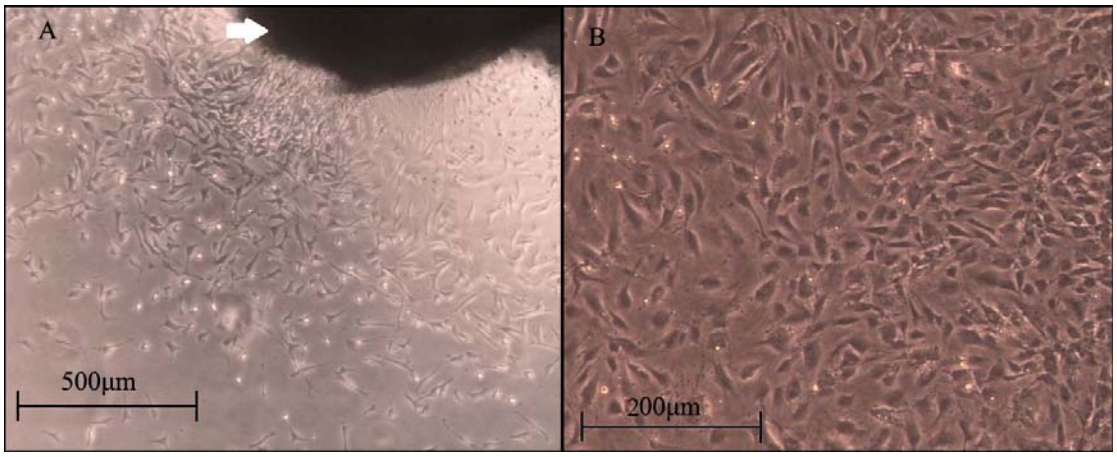

Figure 3.4 *Primary culture of mouse skin fibroblast (A) at 2-3 days depicts outgrowth of cells from the skin explant (white arrow) and (B) the culture at 13-14 days depict the cells at approximately 75% confluence.*

After the mouse skin fibroblasts in a confluent 35mm petri dish were passaged to two T25 tissue culture flasks, the cell monolayer was confluent within 4-5days. On average fibroblast, cell cultures in either T25 or T75 were passaged once a week or when the culture reached 75-85% confluence.

3.3 Cytotoxicity Assays

3.3.1 DAPI/PI Staining

The persistence of ppMWCNT in the stained and fixed samples resulted in counting cell nuclei being problematic for image analysis software. The presence of ppMWCNT appeared to have two effects. First, ppMWCNT at the higher concentrations formed a thin film over the cell monolayer causing a shadow effect that resulted in cell counting by automated methods being inaccurate (see Figure 3.5). Secondly, as ppMWCNT concentrations increased, excitation of propidium iodide decreased resulting in reduced levels of emitted light for image capture.

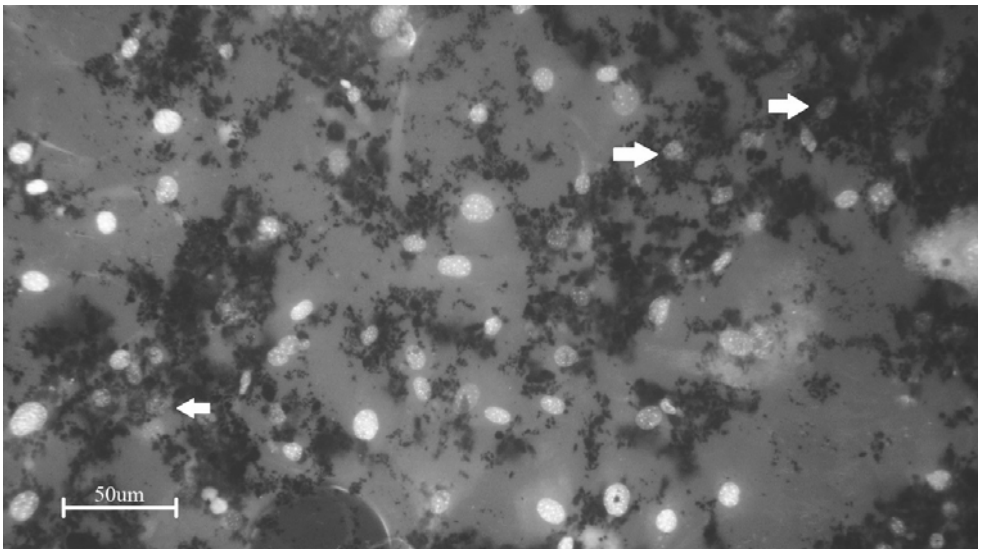

Figure 3.5 *ppMWCNT forming a thin film over DAPI stained nuclei causing a dark shadow. Representative shadowed nuclei are indicated by the white arrows*

In addition to ppMWCNT creating thin films over the fibroblast cells causing interference with excitation and emission of the fluorescent signal, ppMWCNT observably adsorbed PI (as seen in figure 3.6).

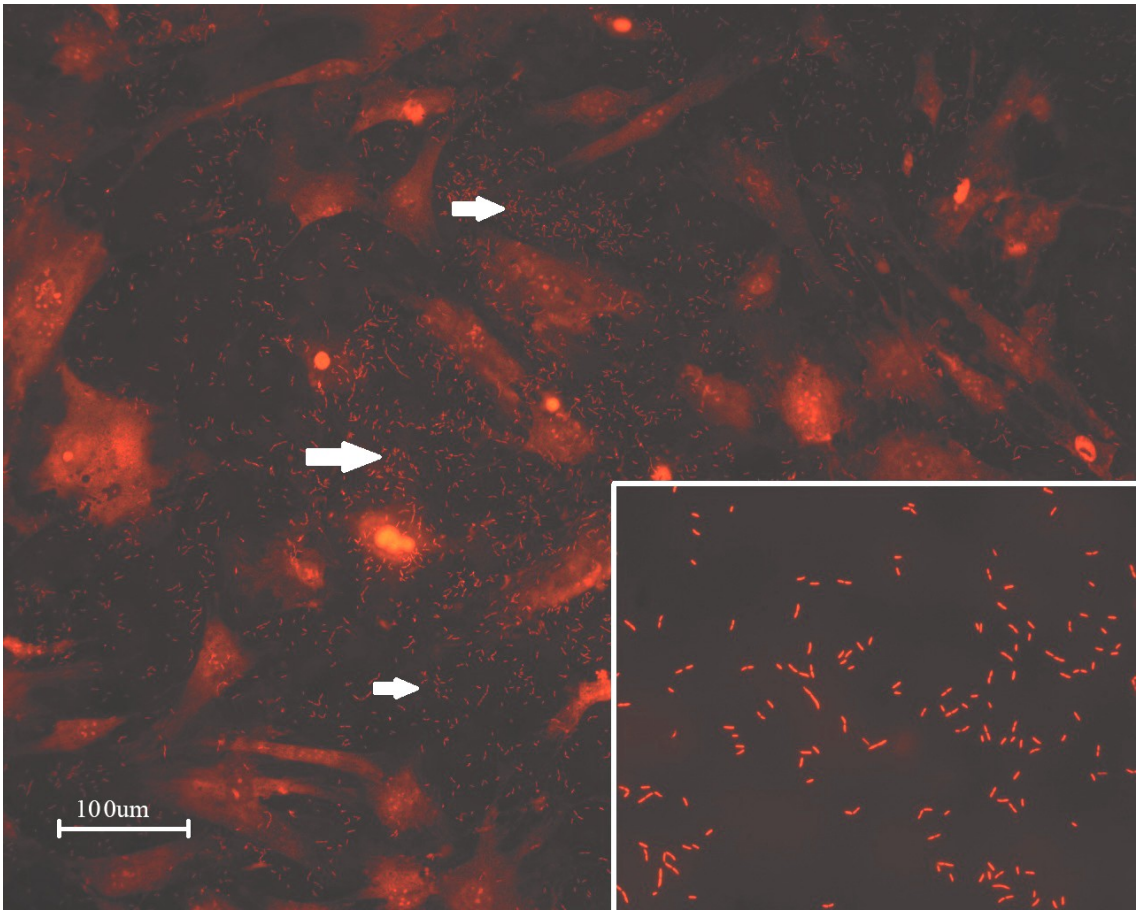

Figure 3.6 *The photomicrograph shows ppMWCNT have adsorbed and emit a red fluorescence (white arrows) characteristic of PI. The image also shows dead fibroblast nuclei (intensely stained red spheres. Inset is an enlargement of ppMWCNT fluorescing red from PI adsorbance.*

DAPI/PI Staining Experimental Results

Table 3.1 Descriptive statistics for percentage viable cells as assessed by DAPI/PI staining

[CNT] Concentration (µg/ml)	Number of repeats per experiment				Mean % viable cells				Std. Error
	Exp 1	Exp 2	Exp 3	Total	Exp 1	Exp 2	Exp 3	Total	
0	20	30	30	80	99.91	99.80	99.84	99.84	0.158
5	20	26	30	76	99.43	99.63	99.72	99.61	0.161
20	20	17	30	67	98.86	99.72	99.03	99.15	0.174
40	29	30	15	74	98.90	99.25	99.30	99.12	0.170
80	30	20	28	78	98.03	98.63	98.23	98.25	0.160
200	20	20	0	40	98.18	98.99		98.58	0.219
500	30	20	0	50	96.34	98.54		97.22	0.200

Live/dead nuclei cell counts obtained following a 6 hour exposure period to increasing concentrations of ppMWCNT indicates a significant ($F(6, 446) = 20.296$, $P<0.001$, $R^2=0.304$) dose dependent trend toward increased cell death (see table 3.1 and figure 3.7).

Percentage of Viable Nuclei Following 6 Hour Exposure to Increasing ppMWCNT Concentrations

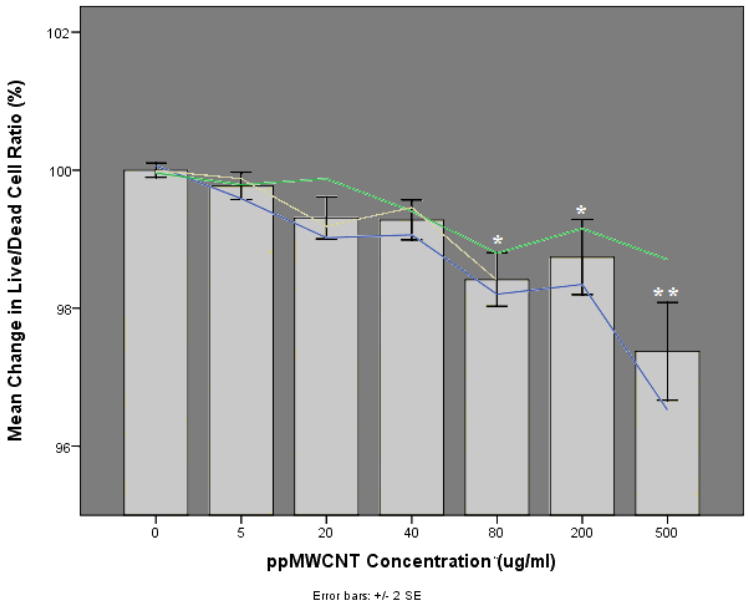

Figure 3.7 *Effect of ppMWCNT concentration on the viability of mouse skin fibroblasts. Bar graph with error bars show the overall effect of increasing ppMWCNT concentration with a trend towards a loss of cell viability (** indicates P=0.001 and * P=0.05 as compared with 0µg/ml). The individual lines represent the mean change in live/dead cell ratio for the three repeats of the experiment. The yellow line ends at 80µg/ml due to a processing error causing 100% cell death across all coverslips in that experimental trial. Values were corrected relative to 0µg/ml = 100% cell viability.*

3.3.2 LDH Cytotoxicity Assay

Pilot Study 1

The potential for ppMWCNT to interfere with light transmission and absorbance in an ELISA plate reader was assessed in a pilot study where the absorbance of varying concentrations of ppMWCNT in FFM 10% was assessed at wavelengths between 400-600nm. The raw data (not shown) indicated there was increasing interference as the ppMWCNT concentration increased.

Pilot Study 2

The results of pilot study 1 identified the need to remove ppMWCNT from the media to enable assessment of LDH using a colorimetric assay. FFM 10% containing ppMWCNT was passed through a 0.45µm syringe filter. Different concentrations of ppMWCNT in FFM 10% LDH with or without LDH present were tested to investigate if ppMWCNT or filtering FFM 10% affected the total measureable LDH levels. The data collected indicate no significant effects (P>0.05) (see figure 3.8).

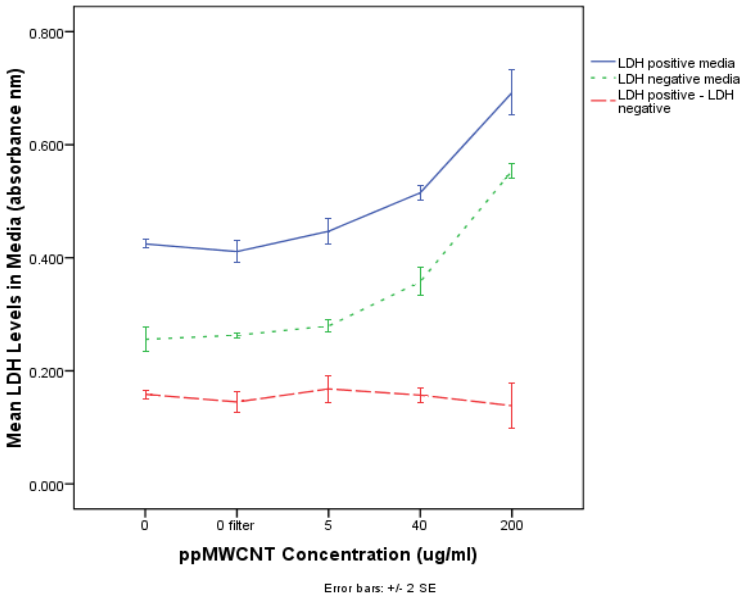

Figure 3.8 *Effect of ppMWCNT concentration on the presence of LDH in FFM 10% (results of pilot study 2). The solid line represents FFM 10% + LDH + ppMWCNT (positive control), the dotted line FFM 10% + ppMWCNT (negative control), and the dashed line (difference of controls) is the product of subtracting the negative control from the positive control (all media was filtered before LDH assay was conducted except for the 0µg/ml sample. This graph indicates that ppMWCNT had no effect on LDH levels or the LDH assay.*

Slight variations in FFM 10% colour after ppMWCNT removal necessitated the use of separate controls for each ppMWCNT concentration used. This was due to incomplete removal of ppMWCNT from the FFM 10% mainly for concentrations of 80µg/ml ppMWCNT and higher (see figure 3.9). The remaining ppMWCNT was enough to affect the light absorbance values obtained at 492nm; however the effect was constant for each concentration so was controllable using LDH free media of the same ppMWCNT concentration.

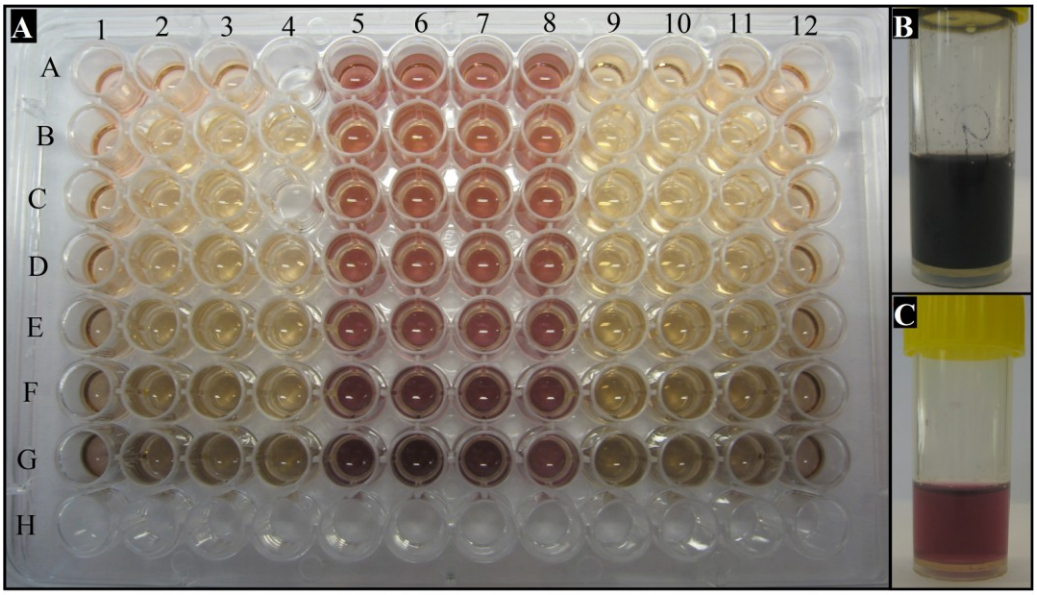

Figure 3.9 *Figure A) is representative of the colorimetric change across the 96 well plate, refer to figure2.2 for contents of each well. Figures B and C are images of the media with 200µg/ml ppMWCNT before (B) and after (C) filtering*

LDH Assay Experimental Results

Changes in LDH levels in fibroblast culture media exposed to increasing concentrations of ppMWCNT indicated an increase in fibroblast cell death ($F(6, 38) = 14.953$, $P<0.001$, $R^2= 0.723$), table 3.2 presents descriptive statistics of the raw data. Concentrations 5-200µg/ml ppMWCNT had significant increases in LDH in the culture media; the level of LDH did not change significantly over the range of ppMWCNT concentrations. At 500µg/ml there was a second significant increase ($P<0.001$) in LDH compared with 0µg/ml and ($P<0.05$) when compared to 5-200µg/ml concentrations (see figure 3.10). Increases in LDH were interpreted as increased cell death.

Table 3.2 Descriptive statistics for changes in cell viability as assessed by LDH assay

[CNT] Concentration (µg/ml)	Number of repeats per experiment			Mean % viable cells			Std. Error
	Exp 1	Exp 2	Total	Exp 1	Exp 2	Total	
0	4	4	8	102.14	101.32	101.71	1.11
5	4	4	8	94.61	97.03	95.83	1.11
20	3	4	7	94.92	93.16	94.05	1.19
40	4	4	8	96.87	94.56	95.72	1.11
80	3	4	7	95.58	95.41	95.50	1.19
200	3	3	6	96.62	93.04	94.84	1.28
500	4	4	8	84.8	89.33	87.07	1.11

Percentage Increase in Extracellular LDH Following 6 Hour Exposure to Increasing ppMWCNT Concentrations

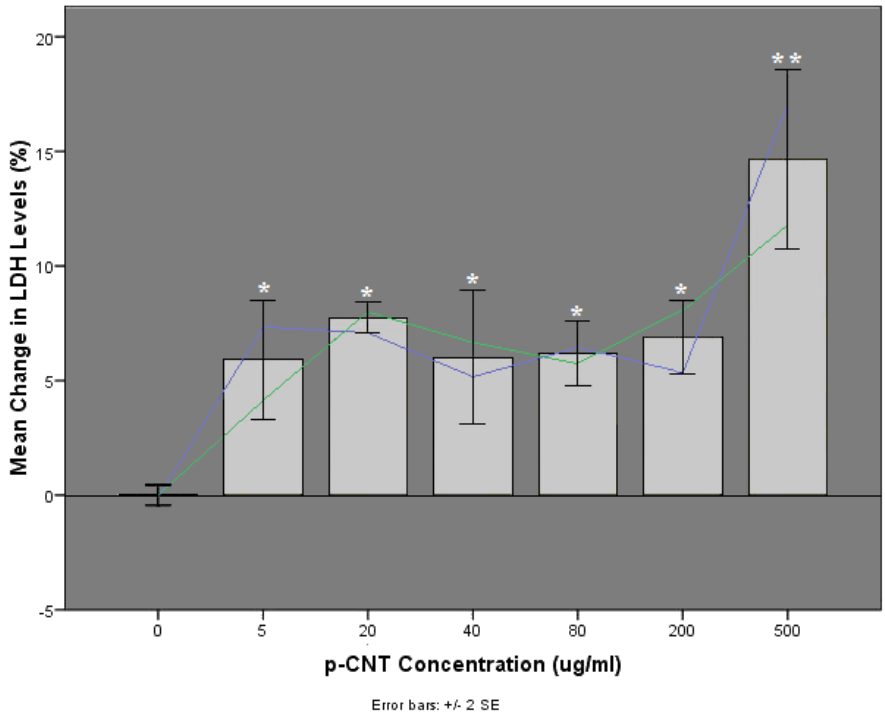

Figure 3.10 *Effect of increasing ppMWCNT on LDH levels in cell culture media (FFM 10%). Bars graph with error bars indicates the overall effect of increasing ppMWCNT concentration on the release of intracellular LDH into the cell culture media (* indicates P=0.05 and ** indicates P=0.001). The line graphs are data from individual experimental trials. Values are corrected relative to 0µg/ml=0% increase in LDH.*

4. Discussion

The potential toxicity of COOH-CNTs is of critical concern. This is due to their proposed use in biomedical applications [4]. It has been suggested that CNTs, both MW and SWCNT, are toxic in vivo [36]. The present study employs a primary cell culture model to assess the cytotoxicity of 250-750nm long, low CCF, acid purified COOH-MWCNT (referred to as ppMWCNT).

The overall aim of the study was to investigate the potential cytotoxicity of carboxylated carbon nanotubes on mammalian cells in vitro. To achieve this goal, three specific sub-aims needed to be met. These aims were:

- To produce a stable, surfactant-free suspension of COOH-CNTs in cell culture media.
- To grow a durable, low maintenance, cell culture model of a widespread cell type.
- To validate two methods of assessing cellular viability/cytotoxicity for investigating ppMWCNT cytotoxicity in vitro.

The initial discussion focuses on the overall results of the present study, regarding the potential cytotoxicity of post processed MWCNT (ppMWCNT) on mammalian cells in vitro. This is followed by specific discussion of the sub-aims.

4.1 Effect of ppMWCNT on Cell Viability

There is already evidence to suggest that a number of forms of carbon nanotube have some degree of cytotoxicity after 12-24 hours in vitro [36]. In the present study, a 6 hour incubation time was chosen to investigate if there was the potential for cytotoxicity to occur in a time frame less than 12 hours.

Carboxylated MWCNT ranging in length from 250 to 750nm suspended in a surfactant-free media caused a significant decrease in fibroblast cell viability in vitro at all concentrations as assessed by DAPI/PI staining and LDH colorimetric assay. The dose-dependence was only significant at ppMWCNT concentrations >80µg/ml for DAPI/PI and >200µg/ml for LDH. Fibroblast cell death increased with increasing ppMWCNT concentration (see figures 3.7 and 3.10). Similar results were reported for both pristine and carboxylated MWCNT 1-5µm in length [5], which showed time and dose dependent

decreases in the viability of human T lymphocytes and Jurkat T leukaemia cell types. Studies by Walker, et al. (2009)[69] identified dose dependent decreases in the viability of human aortic endothelial cells (HAEC) exposed to MWCNT and SWCNT with trace metal concentrations >5% and large agglomerates of CRaP attached to the nanotubes. Additionally Simon-Deckers, *et al*. (2008)[60] using A549 cells (human type II lung epithelium cell line) identified that cytotoxicity of MWCNT increased in a dose dependent manner[60].

4.2 Suspending Carboxylated Multiwalled Carbon Nanotubes

A significant problem that has interfered with CNTs producing stable dispersions in aqueous cell culture media is the physiochemical attraction between CNTs, causing aggregation via van der Waals forces [61]. Methods to disperse CNTs have employed various surfactants [14], protein coatings [10], varying concentrations of serum [13] and protein in the media [43] and covalent functionalization [17] of the CNT itself. It is suggested by Smart, et al. (2006)[61] that the use of various surfactants and CNT modifications alters the way the CNT interacts with cultured cells. Additionally Wick, *et al*. (2007) [72] indicate that the degree of CNT aggregation versus CNT dispersion plays a significant role in CNT cytotoxicity with highly aggregated samples causing greater cell death. The purpose of my study was to assess the potential cytotoxicity of ppMWCNT in fibroblast cell cultures using a cell culture media that provides optimal growth conditions for the cells, without surfactants.

4.2.1 'As purchased' COOH-MWCNT

The suspension of acid purified MWCNT in a cell culture media containing 10% FBS at 1mg/ml was suggested by Vippola et al (2009) [68] to be the most effective way to suspend purified CNTs without surfactants. The use of FBS to suspend CNTs is theorised to work by the proteins being adsorbed directly onto the CNT surface [58] through interactions between the aromatic portions of the protein and the hydrophobic regions of the CNT resulting in a soluble product (see figure 4.1a). Conversely, it has been suggested that the protein, upon sonication, becomes partially denatured exposing the hydrophobic regions of the serum proteins, which then wrap around the CNT [43] (see figure 4.1b). The exact mechanism of the CNT-protein interaction is not yet known. However, the adsorption or wrapping of the protein around CNTs is thought to have two

effects. First, it reduces the size of CNT aggregates in solution. Second, it enhances their dispersion in surfactant free media by encasing the CNTs so that only hydrophilic regions are exposed [68, 70].

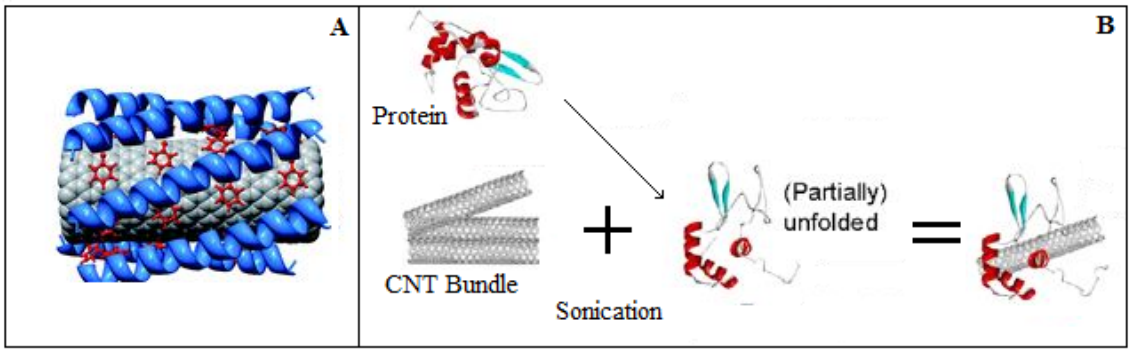

Figure 4.1 *Schematic representation of CNT with proteins adsorbed to outer surface (A) and the wrapping of individual proteins around CNT (B). Figure 'A' is modified from Wallace, et al. (2010)[70] and Figure' B' is modified from Matsuura, et al. (2006)[43].*

However, suspending 'as purchased' 1-5µm COOH-CNTs (obtained from NanoLab) at 1mg/ml in a surfactant free media in the present study formed only a temporary dispersion of aggregated nanotubes that rapidly settled out of suspension. Thus, we used NaOH to increase the potential solubility of the COOH-CNTs through the modification of the COOH group (*personal communication, A. Partridge, 2009*) as shown in figure 4.2. It follows that NaOH reacts with the OH/O^- terminal of the COOH group resulting in an O^-Na^+ terminal altering the hydrophobic nature and increasing the solubility of COOH-CNTs [56].

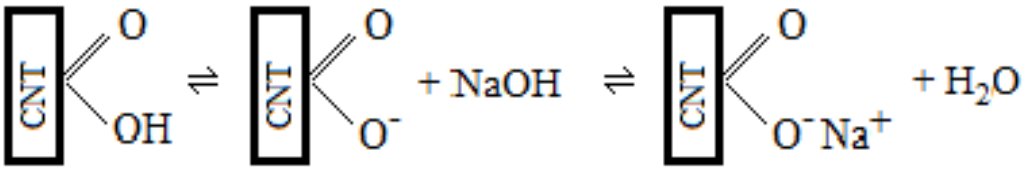

Figure 4.2 *Schematic of the reaction of COOH-CNT with NaOH. Dispersing COOH-CNT in a 1M NaOH solution changes the COOH terminal to COO^-Na^+ making the terminal non-polar and subsequently reducing the hydrophobic nature of the COOH-CNT*

As the results indicated a 1M solution of NaOH resulted in a well dispersed suspension of the 'as purchased' COOH-MWCNT. However, the NaOH solution is strongly basic, which is not compatible with biological systems. Two methods were employed to make the NaOH modified COOH-MWCNT biocompatible. First, NaOH suspension of COOH-MWCNT was centrifuged, the surfactant removed with a glass pasture pipette, and the remaining product resuspended in FFM 10%. The second method directly

diluted the NaOH COOH-MWCNT suspension with FFM 10%. Both methods resulted in unstable suspensions with large aggregates.

Several papers indicated that when CNTs are acid treated, the carboxyl groups form primarily on carbonaceous fragments that are already present, or on fragments that are produced upon the breaking of CNTs at defect sites [18, 56, 58, 71] (See figure 4.3). Further, it is these CCF that contribute significantly to the COOH-CNT insolubility [56]. Based on these observations the 'as purchased' COOH-MWCNT were post-processed to investigate if CCF were present and if the post-processing had an effect on COOH-MWCNT solubility.

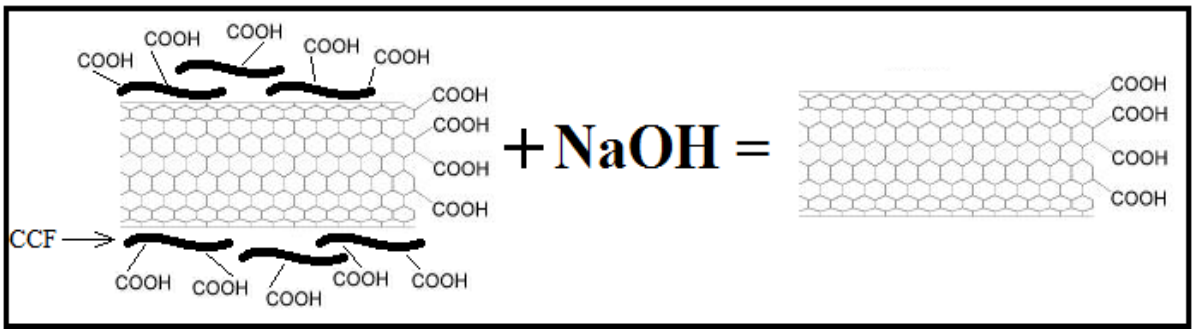

Figure 4.3 *Schematic representation of a SWCNT surrounded by carboxylated carbonaceous fragments (CCF). Upon reflux with 1M NaOH, the OH terminal is changed to O^-Na^+ which solubilises the fragments in the NaOH solution.*

4.2.2 Post Processing MWCNT

The post processing method used is based on the same principle reaction stated above converting the OH terminal of the COOH group to COO^-Na^+, however this was performed using a reflux reaction setup to enhance the access of NaOH to all COOH groups within CNT aggregates. The solubilised CCF were then removed by centrifugation and vacuum filtration[56]. The supernatant collected after centrifugation was dark yellow/brown in colour indicating the presence of solubilised CCF; this agrees with the results of other researchers using similar methods [18, 56, 58].

After CCF content was reduced by consecutive NaOH washes, Na^+ residues remained on COOH groups that were bound to the CNT itself [74]. The presence of the Na^+ ions can have a significant impact by decreasing the pH of later suspensions [24]. Additionally, there were significantly fewer COOH groups surrounding the CNT [71] after the NaOH treatment. Therefore, the CCF reduced CNT sample was refluxed with

HNO_3 firstly to reduce Na^+ residues and to introduce new COOH groups onto the CNT [56], resulting in ppMWCNT used for subsequent in vitro toxicity investigations.

Reacting the NaOH treated CNTs with HNO_3, in addition to its effects above, caused further breakage and degradation of the CNTs at defect sites resulting in shorter, ppMWCNT compared to 'as purchased' MWCNT (see figure 3.1) [56]. Shorter CNTs have been identified as possibly being less cytotoxic compared to longer CNTs [57]. In conjunction with changes in CNT length, TEM images showed a reduction in other CRaP that were present in the 'as purchased' sample.

The COOH-MWCNT sample collected after post processing formed a well dispersed suspension in FFM 10% and the suspension was also stable for up to 24 hours before any sedimentation was observed. Comparing 1mg/ml suspensions of 'as purchased', NaOH treated and ppMWCNT indicated that the processing of the 'as purchased' MWCNT lead to improved dispersion and stability. Therefore, it is concluded that a combination of reduced CCF content [18, 56, 58, 71] the introduction of COOH groups [37] bound directly to the MWCNT and shorter length [24] all have a role in the dispersion and stability of suspensions in FFM 10%.

4.3 Fibroblast Cell Cultures

The methodology used to produce a mouse, skin, fibroblast cell model for toxicity assays from primary explants is similar to protocol 11.4 Freshney (2000) [20]. The fibroblast cell model was chosen as fibroblasts are a widespread cell type that occur throughout the mammalian body [6]. Maintenance and preparation of the mouse skin fibroblasts from primary explant to toxicity assay was a basic, straight forward procedure.

4.4 Cytotoxicity Assays

4.4.1 DAPI/PI Staining

Cell cultures were co-labelled with PI (red) and DAPI (blue) fluorescent probes, DAPI indicated total cell numbers [32, 63] and PI total non-viable cells [19]. DAPI and PI fluorescent probes were chosen for this application, as they are inexpensive and easy to use. The counter-staining method was effective for assessing cell viability of the adherent fibroblast cell cultures. The data collected about individual cell viability using

DAPI/PI agreed strongly with the data obtained from the LDH assay (discussed below). Interestingly, Pulskamp, et al (2007) [51] report that the MWCNT tested at 5, 10, 50 and 100μg/ml showed little to no cytotoxicity to rat alveolar macrophages as indicated by PI/annexin V after 24 hours exposure as counted with fluorescent assisted cell sorting (FACS). Results of the current study indicated that cytotoxicity was significant at 80μg/ml as assessed by DAPI/PI and at 5μg/ml when LDH was assessed. Conversely Pulskamp, et al (2007) [51] also report significant decreases in mitochondrial membrane potentials at all concentrations tested which is supported by the subsequent but not significant dose dependent increases in IL-8 when cell were exposed to 95% pure MWCNT.

As noted in section 3.3.1 after FFM 10% containing ppMWCNT was removed a residual, thin, patchy film of ppMWCNT remained adherent to the unfixed cell cultures. This thin film caused a shadow-like effect (see figure 3.5). The presence of the residual ppMWCNT on samples has three potential explanations. First, the method of rinsing the live cultures before the application of stains and fixing was ineffective, however implementing a more thorough rinsing protocol of live adherent cell can have two possible effects. It could, induce more cell death than that caused by the specific treatment. It could also, remove weakly adherent non-viable cells reducing total number of non-viable cells. Second, the ppMWCNT might interact with the PLL coating on the glass coverslips, used to promote cell adhesion. The amino acid chains present on the PLL could potentially have covalent interactions with the carboxyl groups on the ppMWCNT [76]. A third explanation is, the ppMWCNT were potentially located in the cytoplasm [60, 73] or were membrane bound [69], making rinsing ineffective for removing individual ppMWCNT.

The third explanation derives support from the both the LDH assay and previous research using TEM visualise the location of CNT in cells after exposure [46, 52, 60, 69]. The LDH assay measures the total level of LDH that has been released from cellular cytoplasm resulting from membrane damage. Previous research using TEM provides evidence that the cytoplasmically located CNTs are not bound within vacuoles but are freely distributed within the cytoplasm [46, 60, 69]. This evidence points toward CNT penetrating the cell membrane, which is likely to create pores within the lipid bilayer [67]. A unique property of the present research was the use of a 6 hour treatment period

which is shorter than that used in other experiments. This is relevant as the level of cell death recorded for the higher concentrations of ppMWCNT exposure caused significant increases in cell death in a relatively short period. This combination of results indicates that a primary cause of cell death in vitro is potentially by direct penetration of the cell membrane allowing the leakage intracellular materials such as LDH and providing access for membrane impermanent PI to the cell nucleus within the 6 hour exposure period.

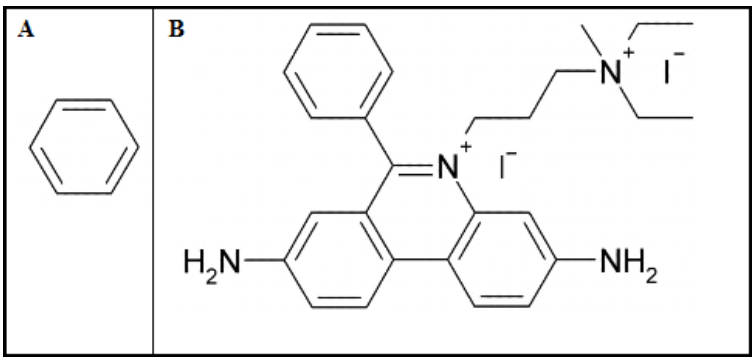

Figure 4.4 *Schematic of a benzene ring (A) and propidium iodide (B). The six membered carbon commonly referred to as a benzene ring is the necessary component making a compound aromatic i.e. contains at least one benzene ring structure. The schematic of propidium iodide indicates that it contains more than one benzene ring therefore making it an aromatic compound.*

The use of PI is common as an indicator of non-viable cells, or an indicator of overall cell numbers (when used after cell permeabilization) in fluorescence microscopy and FACS applications [41]. However, observational data from the current research indicates that there is a potential adsorptive interaction between ppMWCNT and PI resulting in quenching of the red fluorescent signal [31, 46]. It is suggested that compounds that have a large aromatic content are more readily adsorbed onto the surface of CNTs [8]. Aromatics are six membered rings of carbon as shown in figure 4.4a. This hypothesis is supported by Zorbas, et al (2006) [77] where it is indicated that the aromatic content of proteins plays a significant role in protein/CNT interactions. This affinity for the adsorbance of aromatic compounds to the CNT sidewalls could be responsible for the ppMWCNT dose related deterioration in PI excitation and poor emission. This hypothesis is put forward based on the adsorbance of rhodamine B, an aromatic based fluorescent dye, onto CNT sidewalls causing a quenching of Rhodamine B excitation by holding the compound in its ground state through hydrophobic and electrostatic interactions [1].

4.4.2 LDH Cytotoxicity Assay

The processes of apoptosis and necrosis of cells both result in a disruption of the cell membrane releasing the cytoplasmically located enzyme, lactate dehydrogenase. The release of this enzyme can be observed colorimetrically as its presence causes the conversion of a colourless reactant to a coloured product. The measurement of LDH in the cell culture media is a bulk cell assay, as it determines the change in a parameter related to the whole cell population. In contrast, DAPI/PI staining assesses individual cells. Measuring a bulk cell product has advantages over individual cell techniques in terms of time and higher throughput of samples.

Pilot experiments conducted as part of the current research indicated that there were no interactions between the LDH assay used and the ppMWCNT; this result agrees with Wang, et al. (2008) [71]. If an interaction was present, it could have resulted in false positives, as has been reported on several occasions with the MTT colorimetric assay [60, 73, 75].

Walker, et al. (2009) [69] identified a dose dependent increase in LDH when cultures were exposed to MWCNT concentrations between 0.4-4.5μg/ml for 24 hours. The amount of LDH released at these concentrations was higher than observed in other research [51, 60, 75] including the current study. However, we also observed a significant LDH increase at 5μg/ml as compare to 0μg/ml. The effect of ppMWCNT at concentrations ranging from 5-500μg/ml, in the present study, tested for six hour exposure periods indicated significant increases in LDH compared to controls. These data are similar to those recorded by Yang, et al. (2009) [75].

The results obtained from DAPI/PI at the individual cell level agree with the results of the LDH assay at concentrations ≥80μg/ml in the present study. However, DAPI/PI indicates a dose dependent trend for increasing cell death which becomes significant at ≥80μg/ml (see figure 3.7). Whereas the LDH assay identifies significant cell death (P=0.05) at 5μg/ml, this cell death increases with greater significance at 500μg/ml (P=0.001). This data indicates that the LDH assay is a more sensitive method to assess cell death in the presence of ppMWCNT [60]. However, the LDH assay data presented is based on a small number of repeats as seen in table 3.2, this was due to financial constraints and requires further samples to be tested before any solid conclusions can be inferred.

5. Conclusion

This thesis investigates the impact of high purity, low CCF containing, short, carboxylated carbon nanotubes on mammalian cells. Using an in vitro model of a widespread mammalian cell type, the impact of ppMWCNT was assessed with vital staining and colorimetric assay methods. The objective of the investigation was to identify if ppMWCNT at various concentrations were cytotoxic to primary cultured mammalian cells within a 6 hour exposure period. The results indicate that high purity, short, low CCF, COOH-MWCNT, when suspended in cell culture media, without surfactants, are cytotoxic to fibroblast in vitro.

This investigation was performed on the basis that carboxylated carbon nanotubes have been proposed as the primary skeleton nanoparticle for cell targeted, drug and gene carrier vehicles and for non-invasive thermal destruction of cancer. Concurrently, there are concerns about the particle's biocompatibility and propensity to harm living organisms.

The use of DAPI/PI vital staining and LDH colorimetric assay in assessing this interaction indicated a dose dependent cytotoxic relationship in vitro. These data support the hypothesis that carboxylated carbon nanotubes are cytotoxic to mammalian cells in vitro, in a dose dependent manner. This theme of dose dependent toxicity of carbon nanotube materials appears to be common over different cell types and various derivatives of carbon nanotubes.

The most significant limitation of this study was the financial constraints resulting in an incomplete data set for the LDH assay. A minor limitation, with regards to the total time to prepare and analyse samples, was the interference of ppMWCNT with propidium iodide. Further to this, the effect of the residual CNT material on the cell cultures making it difficult to count live cells in each photomicrograph.

The present research indicates a cytotoxic relationship however further research is required to draw solid conclusions. Future work requires modification of the DAPI/PI protocol with regards to cell counting, there is potential to use FACS or similar cell counting methodology reducing the effect of the residual ppMWCNT affecting manual and computerised counting of fluorescent micrographs. In conjunction, more in depth chemical and morphological analysis of the nanomaterial is required. Beyond the scope

of this research, investigations into the route to toxicity of carbon nanotubes would enable better understanding of the potential and the limitations of such a novel material.

Finally, these carboxylated carbon nanotubes should only be considered for biomedical applications with extreme caution as both data from present research and other in vitro and in vivo models, indicate the potential for significant toxicity.

6. References

1. Ahmad, A., et al., (2009) Applications of the static quenching of rhodamine B by carbon nanotubes. *Chemphyschem*. **10**: p. 2251-2255.
2. Arvizo, R.R., et al., (2010) Effect of nanoparticle surface charge at the plasma membrane and beyond. *Nano Letters*. **10**: p. 2543-2548.
3. Banerjee, S., Herraj-Benny, T., and Wong, S.S., (2005) Covalent surface chemistry of single-walled carbon nanotubes. *Advanced Materials*. **17**(1): p. 17-29.
4. Bianco, A., et al., (2005) Biomedical applications of functionalised carbon nanotubes. *Chemical Communications* (5): p. 571-577.
5. Bottini, M., et al., (2006) Multi-walled carbon nanotubes induce T lymphocyte apoptosis. *Toxicology Letters*. **160**(2): p. 121-126.
6. Bourdeau, P., et al., *Non-specialized mammalian cell cultures for toxicity testing*, in *Short-term toxicity tests for non-genotoxic effects*, P. Bourdeau, et al., Editors. 1990, John Wiley & Sons: Chic.
7. Cai, D., et al., (2008) Interaction between carbon nanotubes and mammalian cells: characterization by flow cytometry and application. *Nanotechnology*. **19**: p. 1-10.
8. Chen, W., Duan, L., and Zhu, D., (2007) Adsorption of polar and nonpolar organic chemicals to carbon nanotubes. *Environmental Science and Technology*. **41**: p. 8295-8300.
9. Chlopek, J., et al., (2006) In vitro studies of carbon nanotubes biocompatibility. *Carbon*. **44**(6): p. 1106-1111.
10. Crouzier, T., et al., (2008) Modification of Single Walled Carbon Nanotube Surface Chemistry to Improve Aqueous Solubility and Enhance Cellular Interactions. *Langmuir*. **24**(22): p. 13173-13181.
11. Cui, D.X., et al., (2005) Effect of single wall carbon nanotubes on human HEK293 cells. *Toxicology Letters*. **155**(1): p. 73-85.
12. Dai, H., *Nanotube growth and characterization*, in *Carbon nanotubes: synthesis, structure, properties, and applications*, M.S. Dresselhaus, G. Dresselhaus, and P. Avouris, Editors. 2001, Springer-Verlag: Berlin.
13. Davoren, M., et al., (2007) In vitro toxicity evaluation of single walled carbon nanotubes on human A549 lung cells. *Toxicology in Vitro*. **21**(3): p. 438-448.
14. Dong, L., et al., (2008) Cytotoxicity of single-walled carbon nanotubes suspended in various surfactants. *Nanotechnology*. **19**: p. 255702.
15. Dresselhaus, M.S. and Avouris, P., *Introduction to carbon materials research*, in *Carbon nanotubes: synthesis, structure, properties, and applications*, M.S. Dresselhaus, G. Dresselhaus, and P. Avouris, Editors. 2001, Springer-Verlag: Berlin.

16. Dumitrescu, I., Wilson, N.R., and Macpherson, J.V., (2007) Functionalizing single-walled carbon nanotube networks: Effect on electrical and electrochemical properties. *Journal of Physical Chemistry*. **111**(50): p. 12944-12935.

17. Dumortier, H., et al., (2006) Functionalized carbon nanotubes are non-cytotoxic and preserve the functionality of primary immune cells. *Nano Letters*. **6**(7): p. 1522-1528.

18. Fogden, S., et al., (2008) Purification of single walled carbon nanotubes: The problem with oxidation debris. *Chemical Physics Letters*. **460**: p. 162-167.

19. Foglieni, C., Meoni, C., and Davalli, A.M., (2001) Fluorescent dyes for cell viability: An application on prefixed conditions. *Histochemistry and Cell Biology*. **115**: p. 223-229.

20. Freshney, R.I., *Culture of Animal Cells: A Manual of Basic Technique*. 4th ed. 2000, Chichester: Wiley-Liss.

21. Gannon, C.J., et al., (2007) Carbon nanotube-enhanced thermal destruction of cancer cells in a noninvasive radiofrequency field. *Cancer*. **110**(12): p. 2654-2665.

22. Govindaraj, A. and Rao, C.N.R., *Nanotubes and nanowires*, in *The Chemistry of nanomaterials*, C.N.R. Rao, A. Muller, and A.K. Cheetham, Editors. 2004, Wiley-VCH: Weinheim.

23. Grabinski, C., et al., (2007) Effect of particle dimension on biocompatibility of carbon nanomaterials. *Carbon*. **45**(14): p. 2828-2835.

24. Heister, E., et al., (2010) Higher dispersion efficacy of functionalized carbon nanotubes in chemical and biological environments. *Nano*. **Web**.

25. Helland, A., et al., (2007) Reviewing the environmental and human health knowledge base of carbon nanotubes. *Environmental Health Perspectives*. **115**(8): p. 1125-1131.

26. Hilder, T.A. and Hill, J.M., (2007) Modelling the encapsulation of the anticancer drug cisplatin into carbon nanotubes. *Nanotechnology*. **18**(27): p. 1-8.

27. Hilder, T.A. and Hill, J.M., (2008) Carbon nanotubes as drug delivery nanocapsules. *Current Applied Physics*. **8**(3-4): p. 258-261.

28. Hirsch, A., (2002) Functionalization of single-walled carbon nanotubes. *Angewandte Chemie International Edition*. **47**(11): p. 1853-1859.

29. Hone, J., *Phonons and thermal properties of carbon nanotubes*, in *Carbon nanotubes: synthesis, structure, properties, and applications*, M.S. Dresselhaus, G. Dresselhaus, and P. Avouris, Editors. 2001, Springer-Verlag: Berlin.

30. Iijima, S., (1991) Helical microtubules of graphitic carbon. *Nature*. **354**(6348): p. 56-58.

31. Isobe, H., et al., (2006) Preparation, purification, characterization, and cytotoxicity assessment of water-soluble, transition-metal-free carbon nanotube aggregates. *Angewandte Chemie International Edition*. **45**: p. 6676-6680.

32. Kapuscinski, J., (1995) DAPI: a DNA-specific fluorescent probe. *Biotechnic & Histochemistry*. **70**(5): p. 220-227.

33. Kisin, E.R., et al., (2007) Single-walled carbon nanotubes: Geno- and cytotoxic effects in lung fibroblast V79 cells. *Journal of Toxicology and Environmental Health-Part a-Current Issues*. **70**(24): p. 2071-2079.

34. Klumpp, C., et al., (2006) Functionalized carbon nanotubes as emerging nanovectors for the delivery of therapeutics. *Biochimica Et Biophysica Acta-Biomembranes*. **1758**(3): p. 404-412.

35. Kostarelos, K., (2008) The long and short of carbon nanotube toxicity. *Nature Biotechnology*. **26**: p. 774-776.

36. Lacerda, L., et al., (2006) Carbon nanotubes as nanomedicines - From toxicology to pharmacology. *Advanced Drug Delivery Reviews*. **58**: p. 1460-1470.

37. Lee, j., et al., (2007) Measurement of the dispersion stability of pristine and surface-modified multiwalled carbon nanotubes in various nonpolar and polar solvents. *Measurement Science and Technology*. **18**: p. 3707-3712.

38. Lewinski, N., Colvin, V., and Drezek, R., (2008) Cytotoxicity of nanoparticles. *Small*. **4**(1): p. 26-49.

39. Li, Y., et al., (2004) Purification of CVD synthesized single-walled carbon nanotubes by different acid oxidation treatments. *Nanotechnology*. **15**: p. 1645-1649.

40. Lin, J., et al., (2010) Penetration of lipid membranes by gold nanoparticles: insights into cellular uptake, cytotoxicity, and their relationship. *ACS Nano*. **4**(9): p. 5421-5429.

41. Lin, Y., et al., (2006) Preparation, characterization, and evaluation of immuno carbon nanotubes. *Microchimica Acta*. **152**(3-4): p. 249-254.

42. Louie, S.G., *Electronic properties, junctions, and defects of carbon nanotubes*, in *Carbon nanotubes: synthesis, structure, properties, and applications*, M.S. Dresselhaus, G. Dresselhaus, and P. Avouris, Editors. 2001, Springer-Verlag: Berlin.

43. Matsuura, K., et al., (2006) Selectivity of water-soluble proteins in single-walled carbon nanotube dispersions. *Chemical Physics Letters*. **429**: p. 497-502.

44. Maynard, A.D., et al., (2004) Exposure to carbon nanotube material: aerosol released during the handling of unrefined single-walled carbon nanotube material. *Journal of Toxicology and Environmental Health*. **67**: p. 87-107.

45. Medina, C., et al., (2007) Nanoparticles: pharmacological and toxicological significance. *British Journal of Pharmacology*. **150**(5): p. 552-558.

46. Monteiro-Riviere, N.A., Inman, A.O., and Ryman-Rasmussen, J.P., *Dermal effects of nanomaterials*, in *Nanotoxicology: characterization, dosing and health effects*, N.A. Monteiro-Riviere and C. Lang Tran, Editors. 2007, Informa Healthcare: New York. p. 317-338.

47. Muller, J., et al., (2005) Respiratory toxicity of multi-wall carbon nanotubes. *Toxicology and Applied Pharmacology*. **207**(3): p. 221-231.

48. Muller, J., et al., (2008) Structural defects play a major role in the acute lung toxicity of multiwall carbon nanotubes: toxicological aspects. *Chemical Research in Toxicology*. **21**(9): p. 1698-1705.

49. Nel, A., et al., (2006) Toxic potential of materials at the nanolevel. *Science*. **311**: p. 622-627.

50. Popov, V.N., (2004) Carbon nanotubes: properties and application. *Materials Science & Engineering R-Reports*. **43**(3): p. 61-102.

51. Pulskamp, K.D., S.; Krug, H.F., (2007) Carbon nanotubes show no sign of acute toxicity but induce intracellular reactive oxygen species in dependence on contaminants *Toxicology Letters*. **168**: p. 58-74.

52. Raffa, V., et al., (2008) Can the properties of carbon nanotubes influence their internalization by living cells? *Carbon*. **46**: p. 1600-1610.

53. Raja, P.M.V., et al., (2007) Impact of carbon nanotube exposure, dosage and aggregation on smooth muscle cells. *Toxicology Letters*. **169**(1): p. 51-63.

54. Saito, R., Dresselhaus, G., and Dresselhaus, M.S., *Physical properties of carbon nanotubes*. 1998, London: Imperial College Press.

55. Saito, R. and Kataura, H., *Optical properties and raman spectroscopy of carbon nanotubes*, in *Carbon nanotubes: synthesis, structure, properties, and applications*, M.S. Dresselhaus, G. Dresselhaus, and P. Avouris, Editors. 2001, Springer-Verlag: Berlin.

56. Salzmann, C.G., et al., (2007) The role of carboxylated carbonaceous fragments in the functionalization and spectroscopy of a single-walled carbon-nanotube material. *Advanced Materials*. **19**: p. 883-887.

57. Sato, Y., et al., (2005) Influence of length on cytotoxicity of multi-walled carbon nanotubes against human acute monocytic leukemia cell line THP-I in vitro and subcutaneous tissue of rats in vivo. *Molecular Biosystems*. **1**(2): p. 176-182.

58. Shao, L., et al., (2007) Removal of amorphous carbon for the efficient sidewall functionalisation of single-walled carbon nanotubes. *Chemical Communications*. **47**: p. 5090-5092.

59. Shvedova, A.A., et al., (2005) Unusual inflammatory and fibrogenic pulmonary responses to single-walled carbon nanotubes in mice. *American Journal of Physiology-Lung Cellular and Molecular Physiology*. **289**(5): p. L698-L708.

60. Simon-Deckers, A., et al., (2008) In vitro investigation of oxide nanoparticle and carbon nanotube toxicity and intracellular accumulation in A549 human pneumocytes. *Toxicology*. **253**(1-3): p. 137-146.

61. Smart, S.K., et al., (2006) The biocompatibility of carbon nanotubes. *Carbon*. **44**(6): p. 1034-1047.

62. Son, S.J., Bai, X., and Lee, S.B., (2007) Inorganic hollow nanoparticles and nanotubes in nanomedicine. Part 1. Drug/gene delivery applications. *Drug Discovery Today*. **12**(15-16): p. 650-656.

63. Tarnowski, B.I., Spinale, F.G., and Nicholson, J.H., (1991) DAPI as a useful stain for nuclear quantitation. *Biotechnic & Histochemistry*. **66**(6): p. 296-302.

64. Tian, F.R., et al., (2006) Cytotoxicity of single-wall carbon nanotubes on human fibroblasts. *Toxicology in Vitro*. **20**(7): p. 1202-1212.

65. Torti, S.V., et al., (2007) Thermal ablation therapeutics based on CNx multi-walled nanotubes. *International Journal of Nanomedicine*. **2**(4): p. 707-714.

66. Tran, N.E. and Lambrakos, S.G., (2005) Purification and defect elimination of single-walled carbon nanotubes by the thermal reduction technique. *Nanotechnology*. **16**: p. 639-645.

67. Verma, A. and Stellacci, F., (2010) Effect of surface properties on nanoparticle-cell interactions. *Small*. **6**(1): p. 12-21.

68. Vippola, M., et al., (2009) Preparation of nanoparticle dispersions for in-vitro toxicity testing. *Human & Experimental Toxicology*. **28**: p. 377-385.

69. Walker, V.G., et al., (2009) Potential in vitro effects of carbon nanotubes on human aortic endothelial cells. *Toxicology and Applied Pharmacology*. **236**(3): p. 319-328.

70. Wallace, E.J., et al., (2010) A multiscale stimulation study of carbon nanotube interactions with designed amphiphilic peptide helicies. *Nanoscale*.

71. Wang, Z., et al., (2008) The surface acidity of acid oxidised multi-walled carbon nanotubes and the influence of in-situ generated fulvic acids on their stability in aqueous dispersions. *Carbon*. **47**: p. 73-79.

72. Wick, P., et al., (2007) The degree and kind of agglomeration affect carbon nanotube cytotoxicity. *Toxicology Letters*. **168**: p. 121-131.

73. Worle-Knirsch, J.M., Pulskamp, K., and Krug, H.F., (2006) Oops they did it again! carbon nanotubes hoax scientists in viability assays. *Nano Letters*. **6**(6): p. 1261-1268.

74. Worsley, K.A., et al., (2009) Functionalization and dissolution of nitric acid treated single-walled carbon nanotubes. *Journal of the American Chemical Society*. **131**(50): p. 18153-18158.

75. Yang, H., et al., (2009) Comparative study of cytotoxicity, oxidative stress and genotoxicity induced by four typical nanomaterials: the role of particle size, shape and composition. *Journal of Applied Toxicology*. **29**(1): p. 69-78.

76. Zhang, Y., et al., (2004) Poly-L-lysine functionalization of single-walled carbon nanotubes. *Journal of Physical Chemistry*. **108**: p. 15343-15346.

77. Zorbas, V., et al., (2006) Importance of aromatic content for peptide/single-walled carbon nanotube interactions. *Journal of American Chemical Society*. **127**: p. 12323-12328.

Appendix 1

1.1 Recipes for Cell Culture Media

- Cell culture media was made as required and kept at 2-4˚C for a maximum of 14 days.
- 5ml penicillin (10,000units/ml) and streptomycin (10,000µg/ml) liquid (Invitrogen) was added to each 500ml bottle of DMEM to achieve final concentrations of 100units/ml and 100µg/ml respectively.

Fibroblast Feeding Media 10% (FFM10%) ***[General purpose feeding media]***

88% Dulbecco's Modified Eagle Medium (DMEM) high glucose [4500mg/L] (GIBCO, Invitrogen),

10% fetal bovine serum (GIBCO, Invitrogen, NZ),

2% L-glutamine 200mM [100x liquid] (Invitrogen)

Fibroblast Feeding Media 40% (FFM 40%) ***[Used for reviving cryo-stored cells]***

58% DMEM high glucose [4500mg/L] (GIBCO, Invitrogen),

40% fetal bovine serum (GIBCO, Invitrogen, NZ),

2% L-glutamine 200mM [100x liquid] (Invitrogen)

Cell Freezing Media

10% DMSO (Sigma, NZ)

90% fetal bovine serum (GIBCO, Invitrogen, NZ)

1.2 Fixatives and Stains

Phosphate Buffered Saline (PBS)[non-sterile]

1 packet of PBS pH 7.4 dry powder (Sigma, NZ) was dissolved in 100ml distilled deionised water, the pH was measured with pH meter (EUTECH Instruments, Singapore).

Either 0.1M HCL or 0.1MNaOH was added to adjust the pH (pH=7.4 at room temperature)

4% Paraformaldehyde

1. 400ml 0.01M PBS pH7.4 was warmed to 60-65˚C
2. 16g paraformaldehyde powder (BDH Laboratory Supplies, London, England) was added to the warmed PBS. Approximately 1ml 0.1M NaOH was added to clear the solution.
3. The solution was stirred on a hotplate until completely dissolved.

Propidium Iodide

1. 5mg propidium iodide dry powder (PI) (Sigma Aldrich, NZ) was dissolved in 5ml ddH_2O (Sigma, NZ) to produce a 1mg/ml (1.5mM) stock solution.
2. PI stock solution diluted at 1:200, in Hanks Balanced salt solution (HBSS) [with $MgCl_2$ and $CaCl_2$] (GIBCO, Invitrogen), to produce a working solution of 5µg/ml (7.5µM).

DAPI

1. 5mg DAPI dry powder (4,6-Diamidino-2-phenylindole) (Sigma Aldrich) was dissolved in 1ml ddH_2O (Sigma Aldrich) to produce a 5mg/ml (14.3mM) stock solution.
2. DAPI stock solution was diluted at 1:1000 in ddH_2O (Sigma Aldrich) to produce a working solution of 5µg/ml (14.3µM).

1.3 Poly-L-Lysine (PLL) Coating of Coverslips

PLL Stock Solution

1. 25mg Poly-L-Lysine hydrobromide (PLL) [mol wt = 70,000-150,000] (Sigma) was dissolved in 6.25ml ddH_2O (Sigma) and gently aspirated with 10ml serological pipette to mix, to produce a 4mg/ml PLL stock solution.
2. The dissolved PLL solution was passed through sterile 0.2µm syringe disk filter (Sartorius Stedim Biotech, Aubagne, France) into sterile 5ml Bijoux.

PLL Coating of Coverslips

1. 660µl of PLL stock solution was diluted 1:30.3 in 20ml ddH_2O (sigma) in a 145mm sterile plastic petri dish (NUNC), giving a working solution at 132µg/ml.
2. Autoclaved 13mm glass coverslips (VWR international, Leicestershire, England) were submerged in PLL working solution for 45-60 minutes in 145mm petri dish.
3. 145mm petri dish was swirled at 10 minute intervals to ensure even coating. Simultaneously the solution was checked to ensure that the coverslips were submerged and evenly spread.
4. After 45-60 minutes all PLL working solution was removed to waste container.
5. 10ml ddH_2O was added and swirled to rinse coverslips, then removed to waste.
6. Step 5 was repeated, but only half was removed, to facilitate transfer of coverslips.
7. Using forceps, single coverslips were removed and placed in each well of a 24 well tissue culture plate (Jet Bio-Chemicals INT'L., INC, Canada), and allowed to air dry in class II biological safety cabinet overnight.